

The Carnegie Supernova Project-I: Correlation Between Type Ia Supernovae and Their Host Galaxies from Optical to Near-Infrared Bands*

SYED A UDDIN,¹ CHRISTOPHER R. BURNS,¹ M. M. PHILLIPS,² NICHOLAS B. SUNTZEFF,^{3,4} CARLOS CONTRERAS,² ERIC Y. HSIAO,⁵ NIDIA MORRELL,² LLUÍS GALBANY,⁶ MAXIMILIAN STRITZINGER,⁷ PETER HOEFELICH,⁵ CHRIS ASHALL,⁵ ANTHONY L. PIRO,¹ WENDY L. FREEDMAN,⁸ S. E. PERSSON,¹ KEVIN KRISCIUNAS,³ AND PETER BROWN³

¹*Observatories of the Carnegie Institution for Science, 813 Santa Barbara St, Pasadena, CA, 91101, USA*

²*Carnegie Observatories, Las Campanas Observatory, Casilla 601, La Serena, Chile*

³*George P. and Cynthia Woods Mitchell Institute for Fundamental Physics and Astronomy, Texas A&M University, College Station, TX, 77843, USA*

⁴*Department of Physics and Astronomy, Texas A&M University, College Station, TX, 77843, USA*

⁵*Department of Physics, Florida State University, Tallahassee, FL 32306, USA*

⁶*Departamento de Física Teórica y del Cosmos, Universidad de Granada, E-18071 Granada, Spain*

⁷*Department of Physics and Astronomy, Aarhus University, Ny Munkegade 120, DK-8000 Aarhus C, Denmark*

⁸*Department of Astronomy & Astrophysics, University of Chicago, 5640 South Ellis Avenue, Chicago, IL 60637, USA*

Submitted to ApJ

ABSTRACT

We present optical and near-infrared (*ugriYJH*) photometry of host galaxies of Type Ia supernovae (SN Ia) observed by the *Carnegie Supernova Project-I*. We determine host galaxy stellar masses and, for the first time, study their correlation with SN Ia standardized luminosity across optical and near-infrared (*uBgVriYJH*) bands. In the individual bands, we find that SNe Ia are more luminous in more massive hosts with luminosity offsets ranging between -0.07 ± 0.03 mag to -0.15 ± 0.04 mag after light-curve standardization. The slope of the SN Ia Hubble residual-host mass relation is negative across all *uBgVriYJH* bands with values ranging between -0.036 ± 0.025 mag/dex to -0.097 ± 0.027 mag/dex — implying that SNe Ia in more massive galaxies are brighter than expected. The near-constant observed correlations across optical and near-infrared bands indicate that dust may not play a significant role in the observed luminosity offset–host mass correlation. We measure projected separations between SNe Ia and their host centers, and find that SNe Ia that explode beyond a projected 10 kpc have a 30% to 50% reduction of the dispersion in Hubble residuals across all bands — making them a more uniform subset of SNe Ia. Dust in host galaxies, peculiar velocities of nearby SN Ia, or a combination of both may drive this result as the color excesses of SNe Ia beyond 10 kpc are found to be generally lower than those interior, but there is also a diminishing trend of the dispersion as we exclude nearby events. We do not find that SN Ia average luminosity varies significantly when they are grouped in various host morphological types. Host galaxy data from this work will be useful, in conjunction with future high-redshift samples, in constraining cosmological parameters.

Keywords: supernovae: general, galaxies: fundamental parameters, galaxies: photometry, cosmology: distance scale

Corresponding author: Syed A. Uddin

suddin@carnegiescience.edu

* This paper includes data gathered with the 6.5 meter Magellan Telescopes located at Las Campanas Observatory, Chile.

1. INTRODUCTION

Since the surprising discovery of the accelerated expansion of the Universe (Riess et al. 1998, Perlmutter et al.

1997) using the standardization of SNe Ia (Phillips 1993, Tripp 1998), we have made little progress in understanding the physical cause of this observed acceleration. Although recent results tend to point towards a value consistent with the cosmological constant, other explanations are also possible (see Joyce et al. 2016). Alternative possibilities such as the time-varying nature of dark energy are currently difficult to test due to systematic uncertainties in deriving cosmological parameters (e.g., Betoule et al. 2014, Scolnic et al. 2017). Along with improving photometric calibration, systematics of astrophysical origin need more attention. One such systematic is the interplay between the properties of SNe Ia and their hosts.

A number of studies have been made on the correlation between the properties of SNe Ia and their hosts (Hamuy et al. 1995, Sullivan et al. 2010, Lampeitl et al. 2010, Childress et al. 2013a, Pan et al. 2014, Uddin et al. 2017b, Roman et al. 2018, Wiseman et al. 2020). These studies can be grouped into two categories: global host properties and local host properties (see Uddin et al. 2017b for a review). All studies, with varying degrees of significance, show that on average SNe Ia decline faster and are relatively over-luminous (i.e., more negative values of Hubble residuals¹) after light-curve standardization when hosted in massive galaxies. A few studies show correlations between SN Ia properties and SN Ia–host galaxy separation, as well as morphological types (Wang et al. 1997, Hicken et al. 2009, and Galbany et al. 2012). Some of these studies find that certain subgroups of SNe Ia can be better standard candles based on their host properties (e.g., Rigault et al. 2013, Kelly et al. 2015, Uddin et al. 2017b). Moreover, Uddin et al. (2017a) confirmed there is no bias in cosmological constraints derived from subsamples selected by host properties.

The correlation between SNe Ia luminosities and their hosts currently lacks explanation. A possible suspect is the effect of dust in the host galaxies (Brout & Scolnic 2020). One way to test this is to study SN Ia luminosity–host stellar mass correlations in multiple bands, preferably from optical to near-infrared. All previous studies, except Burns et al. (2018), have used B -band peak brightness to study SN Ia–host correlations. In this study, we derive the properties of host galaxies of SNe Ia

from the *Carnegie Supernova Project-I* (hereafter CSP-I; Hamuy et al. 2006), and study the correlation of SN Ia Hubble residuals in $uBgVriYJH$ bands with these properties. This paper is the first to study SN Ia Hubble residual–host stellar mass correlations from optical to near-infrared wavelengths.

The CSP-I was designed to follow SNe Ia discovered at low redshifts, mostly from targeted transient search programs. The CSP-I performed photometric follow-ups over a wide range of bands from optical to near-infrared ($uBgVriYJH$), and was conducted between 2004–2010. The light-curves of SNe Ia from CSP-I are published in three papers (Contreras et al. 2010, Stritzinger et al. 2011, and Krisciunas et al. 2017). Burns et al. (2018) presented an absolute calibration of CSP-I SNe Ia photometry, and a new measurement of the Hubble constant. The second phase of the CSP (CSP-II) was conducted between 2011–2015, and the resulting SN Ia sample characteristics are described in Phillips et al. (2019) and in Hsiao et al. (2019). Optical and near-infrared Hubble diagrams from a combined SN Ia sample from CSP-I and CSP-II will be presented in a future paper (Uddin et al. in preparation). The purpose of this paper is to present the methodology of host mass determination and apply this to publicly available CSP-I data.

In § 2, we describe the SN Ia and host galaxy sample, § 3 describes host galaxy properties, and § 4 presents correlations between SNe Ia and hosts. A discussion of our findings is in § 5, and we conclude in § 6.

2. DATA

2.1. SN I Light-curves

We fit SN Ia light-curves using SNooPy (Burns et al. 2011). Briefly, the best-observed SNe Ia from the CSP-I are used as a training set to obtain light-curve templates for the set of $uBgVriYJH$ filters as a function of a dimensionless color-stretch parameter s_{BV} ² (Burns et al. 2014). These templates are then used to fit the CSP-I sample of SNe Ia, resulting in estimates of s_{BV} , and magnitudes at maximum in each filter. K -corrections are computed using the SN Ia spectral energy distribution sequence of Hsiao et al. (2007), which are updated to include near-infrared templates. Using the intrinsic colors from Burns et al. (2014), the reddening parameters $E(B - V)_{\text{host}}$ and R_V^{host} can also be determined. Finally, using the absolute magnitudes from Burns et al.

¹ Hubble residual is the difference between the predicted and the observed values of distance moduli after obtaining a best-fit cosmological model for a given set of SNe Ia. We will refer to Hubble residuals as luminosities in such a way that negative values indicate more luminous SNe Ia.

² s_{BV} is defined as the rest-frame time of maximum of the $B - V$ color-curve relative to time of B -band maximum divided by 30.

(2018), we can infer distances and compute Hubble residuals. The Hubble residuals of the CSP-I SN Ia sample used in this work are tabulated in Table A1. The following peculiar SNe Ia from the CSP-I are excluded: SN 2004dt, SN 2005gj, SN 2005hk, SN 2006bt, SN 2006ot, SN 2007so, SN 2008ae, SN 2008bd, SN 2008ha, SN 2008J, SN 2009dc, SN 2009J, and SN 2010ae (for details, see Krisciunas et al. 2017).

2.2. Host Galaxies

We obtain the list of host galaxies of CSP-I SNe Ia from Krisciunas et al. (2017). This is the final data release paper of CSP-I photometry and lists 123 SNe Ia in the redshift range of $0.004 < z < 0.083$. Host galaxy reference images were obtained at sufficiently later times so that no significant contribution of light from the SNe Ia contaminates the photometry. These were obtained primarily using the Tek5 optical CCD camera and the near-infrared RetroCam on the 2.5 m Irène du Pont telescope, as well as with the SITe3 CCD camera on the 1 m Henrietta Swope telescopes at the Las Campanas Observatory. Some near-infrared images were also taken with the FourStar instrument on the 6.5 m Magellan Baade telescope. The reader is referred to Krisciunas et al. (2017) for further details.

In several cases, host identification of the SN Ia remains ambiguous. As described in detail in Krisciunas et al. (2017), the host galaxies of SN 2004gc, SN 2007A, SN 2007if, SN 2007mm, SN 2008bf, and SN 2008ff are unclear. These SNe Ia exploded within groups of galaxies where it is difficult to assign the true host, and so we exclude them from this paper. Also, two SNe Ia share the same host: SN 2006mr and SN 2006dd. We exclude SN 2006dd since it was not observed by the CSP-I until very late epochs, making light curve fitting with SNooPy impossible. Finally, we exclude SN 2007sr as the host galaxy of this SN Ia is NGC 4038/NGC4039, also known as the Antennae Galaxies. SN 2007sr exploded in one of the tidal tails of this interactive pair (Schweizer et al. 2008), which makes it difficult to assign the correct host. Moreover, the field of view of the CCD camera of the du Pont Telescope was not large enough to image this pair of galaxies.

2.3. Host Galaxy Photometry

We measure apparent magnitudes of the host galaxies in each of the *ugriYJH* bands. Before performing photometry, we align all images with respect to the centers of each host galaxy, then co-add multiple exposures to make deeper images. We perform photometry using Source Extractor (SExtractor; Bertin & Arnouts 1996)

in single image mode. We inspect SExtractor check images for failed detection and appropriate deblending. Using calibrated local sequence stars, we determine zero points in each stacked image and compute apparent magnitudes of host galaxies using the MAG_AUTO magnitude definition of SExtractor.

As a check, we compare our optical photometry with the SDSS model magnitudes available from the SDSS Sky Server³, and with near-infrared photometry (*J* and *H*) from the 2MASS all-sky survey extended source catalog⁴. We show these comparisons in Fig. 1 and in Fig. 2, respectively. Slopes of best-fit relations and mean offsets with respect to CSP-I photometry are shown in Table 1.

Table 1. Slopes of best-fit relations and mean offsets when comparing CSP-I photometry with SDSS *ugri* photometry, and with 2MASS *JH* photometry.

| Band | Slope | Offset (mag) |
|----------|-------|--------------|
| <i>u</i> | 0.99 | 0.18 |
| <i>g</i> | 1.00 | 0.05 |
| <i>r</i> | 1.02 | 0.06 |
| <i>i</i> | 1.01 | 0.06 |
| <i>J</i> | 1.04 | 0.03 |
| <i>H</i> | 1.04 | 0.03 |

In some cases, when the host galaxy was not observed in a particular band by the CSP, photometry was obtained from external sources. For optical (*ugri*) filters, SDSS model magnitudes⁵ were used, and for near-infrared (*J* and *H*), 2MASS extended source magnitudes were used. Offsets from Table 1 were applied to convert SDSS and 2MASS magnitudes to CSP-I system. We present photometry of the CSP-I SN Ia host galaxies in Table B1.

3. HOST GALAXY PROPERTIES

3.1. Stellar Mass

The physical properties of the host galaxies are derived by using the Z-PEG (Le Borgne & Rocca-Volmerange 2002) Spectral Energy Distribution (SED) software to fit the *ugriYJH* photometry. We follow the same procedure as described in Uddin et al. (2017b). Z-PEG uses the PEGASE 2.0 (Fioc & Rocca-Volmerange 1997)

³ <https://skyserver.sdss.org/dr12/en/tools/search/IQS.aspx>

⁴ <http://tdc-www.harvard.edu/catalogs/tmxsc.html>

⁵ SDSS recommends the use of model magnitudes for extended objects; details are in <https://www.sdss.org/dr12/algorithms/magnitudes/>

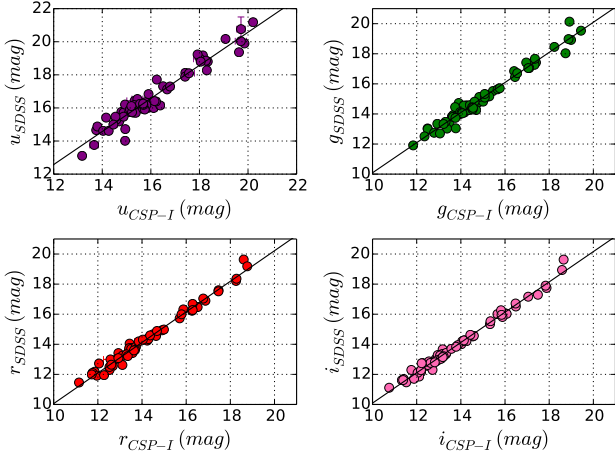


Figure 1. Comparison between host galaxy magnitudes from CSP and SDSS. In each case, solid lines are the best-fit linear relations to the data.

spectral libraries, and computes best matches using χ^2 minimization. There are nine galaxy templates: E, S0, Sa, Sb, Sbc, Sc, Sd, Im, and starburst. Additional internal extinction values are applied to each template ranging from 0.0 mag to 0.5 mag in steps of 0.05 mag. The Rana & Basu (1992) Initial Mass Function was adopted. The stellar masses of the CSP-I host galaxies are shown in Fig. 3 and presented in Table C1. The distribution has a peak at a relatively high mass, which is consistent with the fact that most SNe Ia were discovered by galaxy-targeted supernova searches (Hamuy et al. 2006).

Kelly et al. (2010) demonstrated that galaxy stellar masses determined from multi-band photometry are in good agreement with those derived using galaxy spectra. They considered 10,000 galaxies from the SDSS and found an rms dispersion of 0.15 dex when they compared stellar masses derived using *ugriz* photometry to those using spectral indices. Childress et al. (2013b) also performed a similar analysis and found similar dispersions when comparing 3673 galaxies.

Previously, Burns et al. (2018) calculated host galaxy stellar masses for the CSP-I SNe Ia using 2MASS *K*-band magnitudes. They utilized an empirical relation assuming a constant stellar mass-to-light ratio and normalized to the stellar masses from Neill et al. (2009). The host stellar masses that we calculate from this work are on average 0.3 dex lower than Burns et al. (2018). Comparing the host masses of 25 SNe Ia from this work that are in common with Neill et al. (2009), we find a mean difference of 0.18 dex. This comparison is shown in Fig. 4. It should be noted that Neill et al. (2009) used additional ultra-violet photometry from *GALEX* along

with optical photometry in their analysis. As discussed in Childress et al. (2013b), ultra-violet photometry can be influenced by star-formation histories, and can lead to differences in deriving photometry-based galaxy properties. Only 40% of the host galaxies in this work have photometry from *GALEX*. To maintain consistency we did not use *GALEX* data to derive host properties.

3.2. Separation Between SNe Ia and Hosts

We calculate the projected separation between SNe Ia and their hosts. First, we compute angular separations between SNe Ia and the center of their respective hosts. Then we calculate the distance to each SN Ia using redshift and an assumed value of the Hubble-Lemaître constant, $H_0 = 70 \text{ km sec}^{-1} \text{ Mpc}^{-1}$. With these, we calculate a projected distance in kiloparsecs.

4. SN IA - HOST CORRELATIONS

4.1. $\Delta m_{15}(B)$ and s_{BV}

In this section, we present correlations between SNe Ia properties and their host galaxies. We take SN Ia properties such as *B*-band decline rate, $\Delta m_{15}(B)$ ⁶, color-stretch parameter, s_{BV} , and Hubble residual, $\Delta\mu$, from Burns et al. (2018). In Fig. 5 we show how $\Delta m_{15}(B)$ and s_{BV} correlate with host stellar mass. We do not see strong correlations, but as first noted by Sullivan et al. (2010), massive hosts are observed to produce SNe Ia over the full range of decline rates, whereas less massive hosts preferentially give rise to slower declining events. We compare SN Ia light-curve properties with host galaxy (*g*−*r*) color in Fig. 6, where SN Ia properties are now on the horizontal axis. We reproduce the results in Hamuy et al. (2000) who found that fast declining SNe Ia are missing from blue galaxies with $(B - V) \leq 0.7$ mag, whereas galaxies with $(B - V) \geq 0.7$ mag produce SNe Ia with a wider range of decline rates. We see a similar pattern in our work, with the division occurring at $(g - r) \sim 0.6$ mag. We also find an excess of SNe Ia with higher values of s_{BV} (lower values of $\Delta m_{15}(B)$) occurring in bluer galaxies. Finally, we label galaxies with their morphological information obtained from NASA Extragalactic Database (NED)⁷. These classifications are available for 75% of CSP-I SN Ia host galaxies. Hamuy et al. (1995, 1996, 2000) found that spiral galaxies preferentially produce slower declining SNe Ia,

⁶ $\Delta m_{15}(B)$ is defined as the difference in magnitude of the *B*-band light-curve between maximum and day 15 in the rest-frame of the SN Ia (Phillips 1993).

⁷ <http://ned.ipac.caltech.edu>

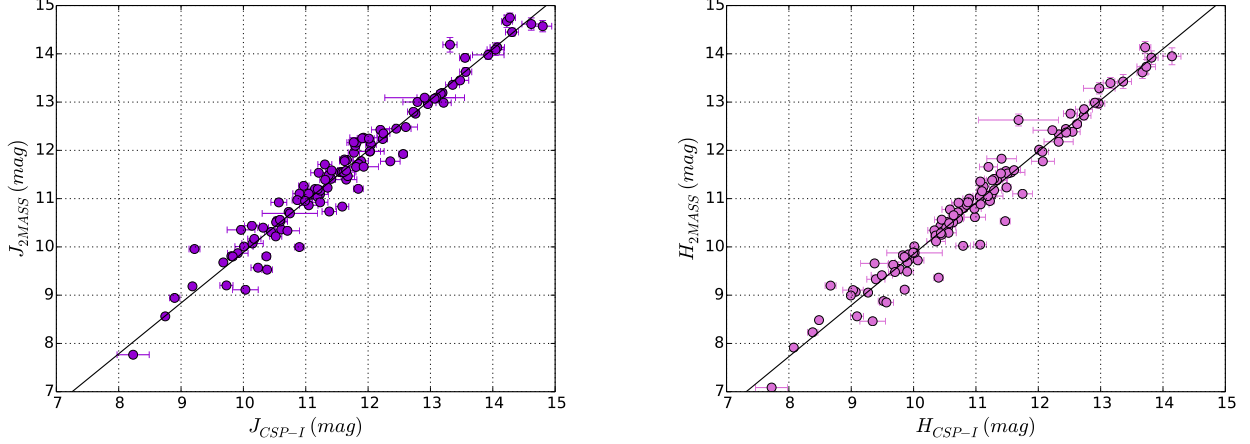


Figure 2. Comparison between host galaxy magnitudes from CSP-I and the 2MASS extended source catalog. In each case, solid lines are the best-fit linear relations to the data (see Eqn. 2).

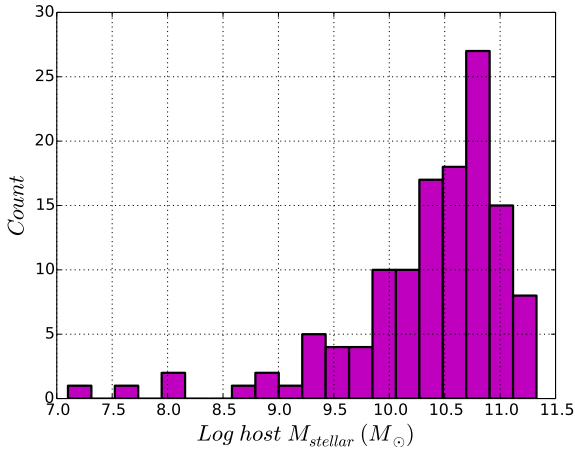


Figure 3. Distribution of host galaxy stellar mass of SNe Ia from CSP-I. The distribution has a peak at a relatively high mass, which is a consequence of galaxy-targeted SN Ia searches.

whereas elliptical galaxies mostly host faster declining events. In order to test this, we perform a Kolmogorov-Smirnov (K-S) test to study possible intrinsic differences between the two populations of CSP-I SNe Ia: those exploding in spiral galaxies and those in elliptical or S0 galaxies. In terms of $\Delta m_{15}(B)$, the K-S test gives a value of 0.13 for D -statistics⁸ and a p -value of 0.47. For this value of D -statistics, the confidence level, $c(\alpha)$, is smaller than 0.005. Since p -value $\gg c(\alpha)$, we reject the null hypothesis — that is, the two samples are likely drawn from the same population.

⁸ D -statistics is the maximum difference between two cumulative distributions.

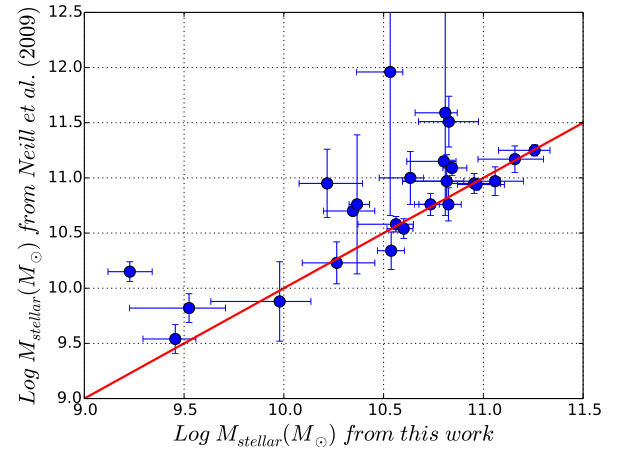


Figure 4. Comparison of host stellar masses from CSP-I and Neill et al. (2009). The solid line shows the one-to-one relation. Neill et al. (2009) determined, on average, 0.18 dex higher mass than what we calculate in this work. See text for discussion.

4.2. Hubble Residuals ($\Delta\mu$)

While the relations between $\Delta m_{15}(B)$ and s_{BV} with host properties are important from an astrophysical point of view (e.g., the explosion mechanism), SN Ia standardized luminosity variation with host stellar mass is important in deriving cosmological parameters (see Uddin et al. 2017b). In this section, we explore correlations between host stellar mass and SN Ia Hubble residuals for each of the $uBgVriYJH$ filters employed by the CSP-I, as shown in Fig. 7.

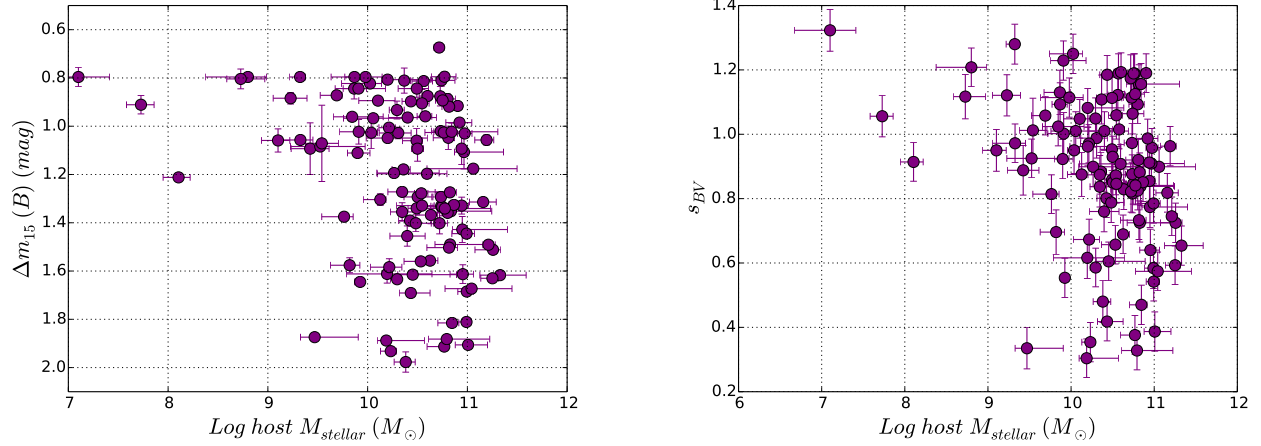


Figure 5. Distribution of $\Delta m_{15}(B)$ and s_{BV} with respect to their host stellar mass. See text for discussion.

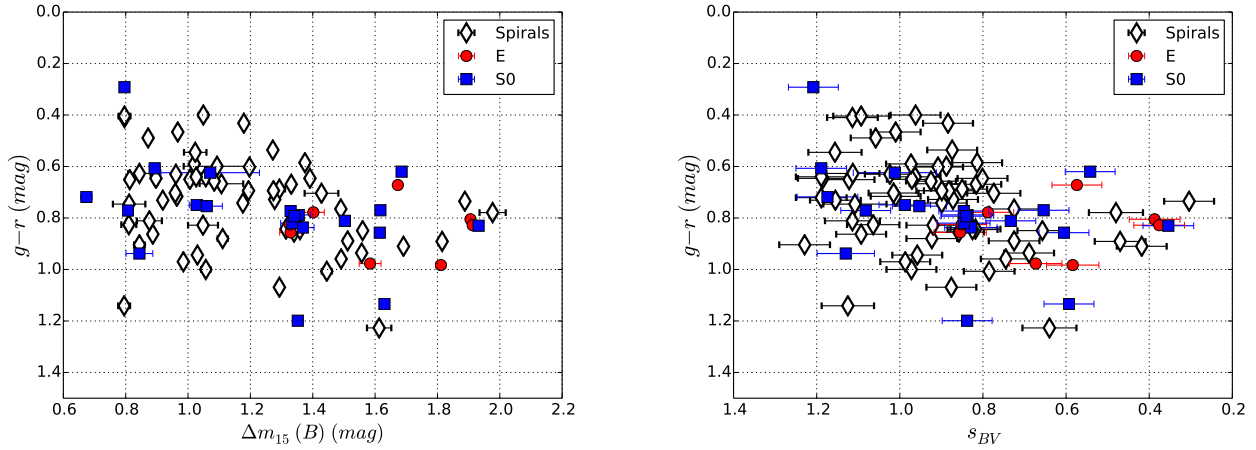


Figure 6. Distribution of $\Delta m_{15}(B)$ and s_{BV} with respect to their host $(g-r)$ color. See text for discussion.

To quantify these correlations, we first calculate slopes of linear fits using the Orthogonal Distance Regression⁹ from the SciPy package. This technique takes into account errors on both axes while performing a functional fit through the data. Slopes are found to be negative across all filters, implying that SNe Ia in more massive galaxies are brighter than expected after standardizing the peak magnitudes using the luminosity–decline rate relation. The slope is least negative in V -band with a value of -0.036 ± 0.025 mag/dex and most negative in Y -band with a value of -0.096 ± 0.027 mag/dex. Table 2 summarizes the values of the slopes. While the slopes vary from filter to filter, these variations do not deviate significantly from a constant value.

Next, we split our sample into two groups at the median value of host stellar mass, $\log M_{\text{stellar}}(M_{\odot}) = 10.48$, and compute the weighted mean of Hubble residuals in each group. We find, on average, that SNe Ia that explode in a host at a higher mass than the median are over-luminous, after light-curve standardization. We call this the Hubble residual offset, Δ_{HR} . The offset varies across the filters, ranging from -0.074 ± 0.030 mag to -0.147 ± 0.040 mag. Table 2 summarizes the values of Δ_{HR} . Negative values of Δ_{HR} indicate that SNe Ia are more luminous in massive hosts. Note that the values of the slopes that we calculate are consistent within the uncertainties with those obtained by Burns et al. (2018).

SNe Ia in the nearby universe are affected by peculiar velocities, which in turn affects both SN Ia luminosities and host galaxy stellar mass in a correlated manner. We might, therefore, expect these correlations to

⁹ <https://docs.scipy.org/doc/scipy/reference/odr.html>

change when nearby SNe Ia are excluded. Figures 8 and 9 display the correlations after excluding SNe Ia with redshifts $z < 0.005$ and $z < 0.01$, respectively. Table 2 summarizes the slopes and Δ_{HR} values obtained in different filters after applying these redshift cuts, with the results displayed visually in Fig. 10. We find that the slopes shift towards positive values, but these shifts are not significant. The Δ_{HR} values change even less after excluding nearby SNe Ia.

Finally, we investigate two special cases. Typically, fast decliners and heavily reddened SNe Ia are not included in most cosmological analyses. To test how the SN Ia Hubble residual-host mass correlations might change by excluding these objects, we eliminate all SNe in the CSP-I sample with $s_{BV} > 0.5$ and $E(B - V) < 0.5$ mag. The resulting sample is plotted in Fig. 11 and slopes and Δ_{HR} are included in Table 2. We find small shifts in the values of the slopes and Δ_{HR} , but these are consistent within the errors with the values obtained for the full sample.

The CSP-I sample includes several SNe identified as 91T- and 91bg-like events. These classification are from Folatelli et al. (2013), and are based on spectral comparison with SNID templates (Blondin & Tonry 2007). The Hubble residual-host mass correlations without these objects are plotted in Fig. 12, and the resulting slopes and Δ_{HR} values are included in Table 2. Again, we find only small shifts in these values.

It is important to note that the correlation between SN Ia Hubble residual and host galaxy stellar mass exists across all filters, *from optical to near-infrared wavelengths*. This implies that differences in the properties of the dust in low- and high-mass host galaxies is not likely the driving factor in these correlations, contrary to what is postulated by Brout & Scolnic (2020).

We further explore this in Fig. 13 where we plot the wavelength-dependence of Hubble residuals one would expect from the Brout & Scolnic (2020) model. These were estimated by randomly drawing a set of 100 color excesses, $E(B - V)$, and values of the ratio of total to selective absorption, R_V , for a low-mass and high-mass sample consistent with the findings of Brout & Scolnic (2020). For $E(B - V)$ we drew from an exponential distribution with scale $\tau = 0.18$ mag for the high-mass sample and $\tau = 0.16$ mag for the low-mass sample. For R_V , we drew from a normal distribution with a mean $R_V = 1.5$ and standard deviation $\sigma_{R_V} = 0.8$ for the high-mass sample, and a mean $R_V = 2.5$ and $\sigma_{R_V} = 2.2$ for the low-mass sample. From these we computed, for each filter, the mean offset in luminosity that would re-

sult from assuming (incorrectly) there was a single average R_V for both samples. As is seen in Fig. 13, the resulting prediction for the behavior of the Hubble residual as a function of wavelength is not a good fit to the CSP-I observations.

4.3. Effect of SN Ia-Host Separation

We also investigate how Hubble residual varies as a function of the positions of the SNe in their host galaxies. This is displayed in Fig. 14 across the *uBgVriYJH* filters. In Table 3, values of the dispersion in Hubble residuals for SNe Ia within 10 kpc of their host centers and for those beyond 10 kpc are tabulated for each filter. We find that SNe Ia exploding farther than 10 kpc from their host centers have a dispersion in Hubble residuals that is smaller than that for the SNe that explode within 10 kpc of their host centers. The reduction in the dispersion for the full sample varies from 30% to 50% across the filters. For the *B* band, which is representative of all the filters, the dispersion in Hubble residual for the SNe Ia beyond 10 kpc projected distance is ~ 0.1 mag smaller than the dispersion for the SNe Ia within 10 kpc.

We perform a Kolmogorov-Smirnov (K-S) goodness-to-fit test to study possible intrinsic differences between these two populations, one within 10 kpc projected distance, and the other beyond 10 kpc projected distance. The K-S test gives a value of 0.257 for *D - statistics* and a *p - value* of 0.218. For this value of *D - statistics*, the confidence level, $c(\alpha)$, is smaller than 0.001. Since *p - value* $\gg c(\alpha)$, we reject the null hypothesis - that is, the two samples are likely drawn from the same population.

We note that there are 20 SNe Ia beyond 10 kpc from their host centers, perhaps causing a biased result due to small number statistics. To check this possible bias and verify our finding, we perform a Monte Carlo simulation. The steps are: 1.) we first calculate the standard deviation of Hubble residuals for 20 SNe Ia that are beyond 10 kpc from their host centers; 2.) we randomly draw 20 SNe Ia Hubble residuals from SNe Ia that are within 10 kpc from their host centers and calculate the standard deviation; and 3.) we compare the standard deviations of the Hubble residuals found in steps 1 and 2. After running a million Monte Carlo realizations in this manner, the mean of the differences in the standard deviations is found to be 0.12 ± 0.03 mag. This implies that the result we have found did not occur by chance.

To check if the peculiar velocities of nearby SNe Ia have an effect, we recalculate the dispersions in Hubble residual for SNe Ia at $z > 0.005$ and at $z > 0.01$ (see Table

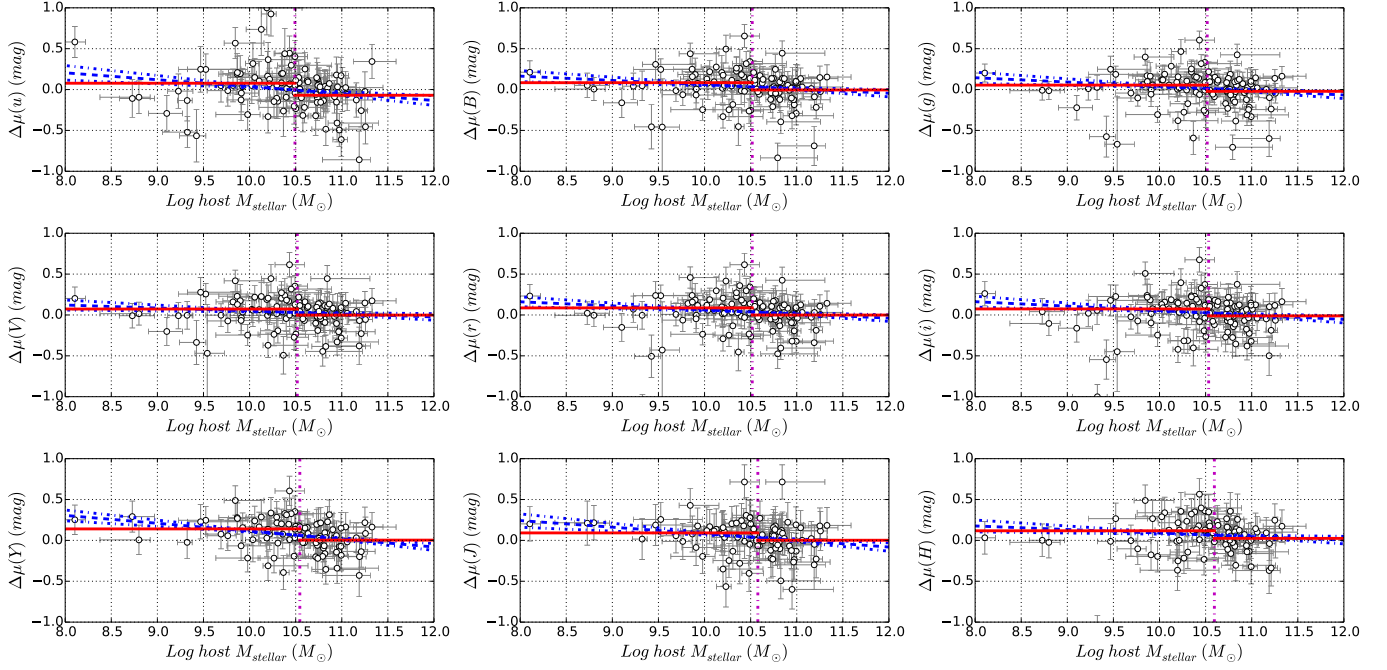


Figure 7. SN Ia Hubble residual ($\Delta\mu$) vs host stellar mass across *uBgVriYJH* bands. In each case, the vertical magenta dash-dotted line shows the median split point, the slanted blue dashed line shows the best-fit linear trend with uncertainties in blue dash-dotted lines, and the red solid line shows the weighted mean of Hubble residuals at both sides of the split point. Slopes of the best-fit lines and Hubble residual offsets are presented in Table 2.

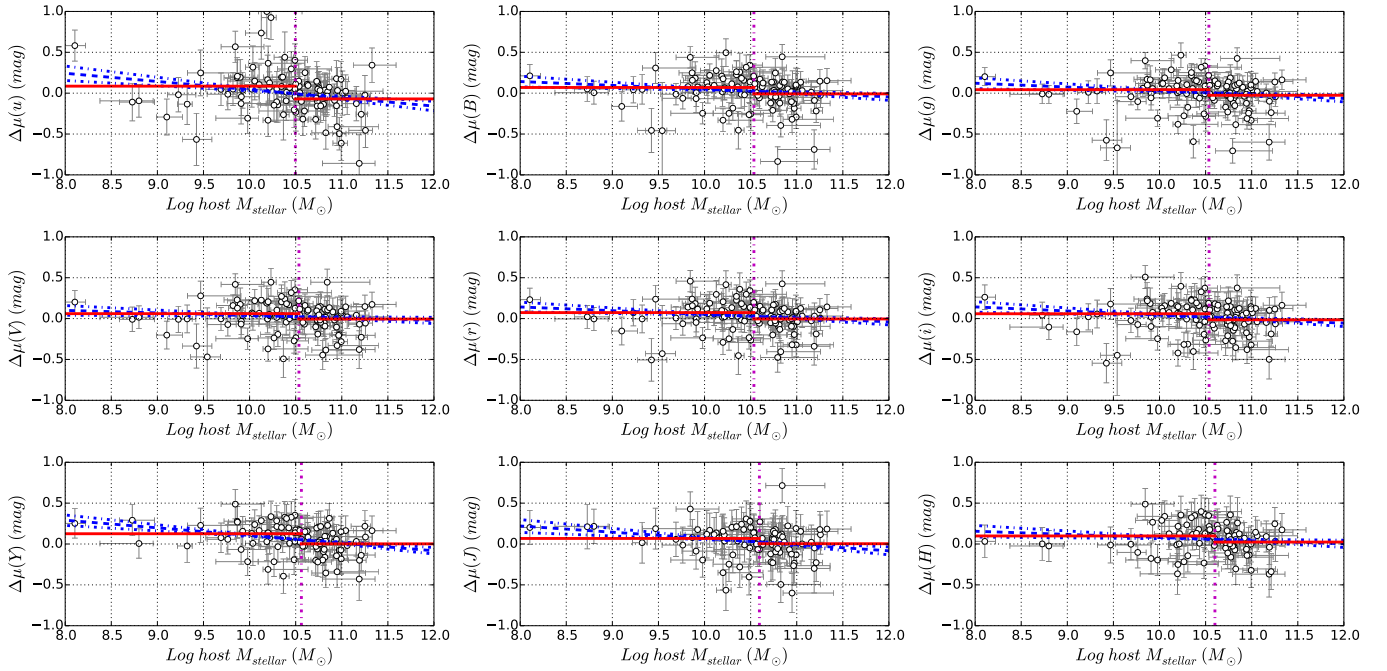


Figure 8. Same as Fig. 7 but including SNe Ia with $z > 0.005$.

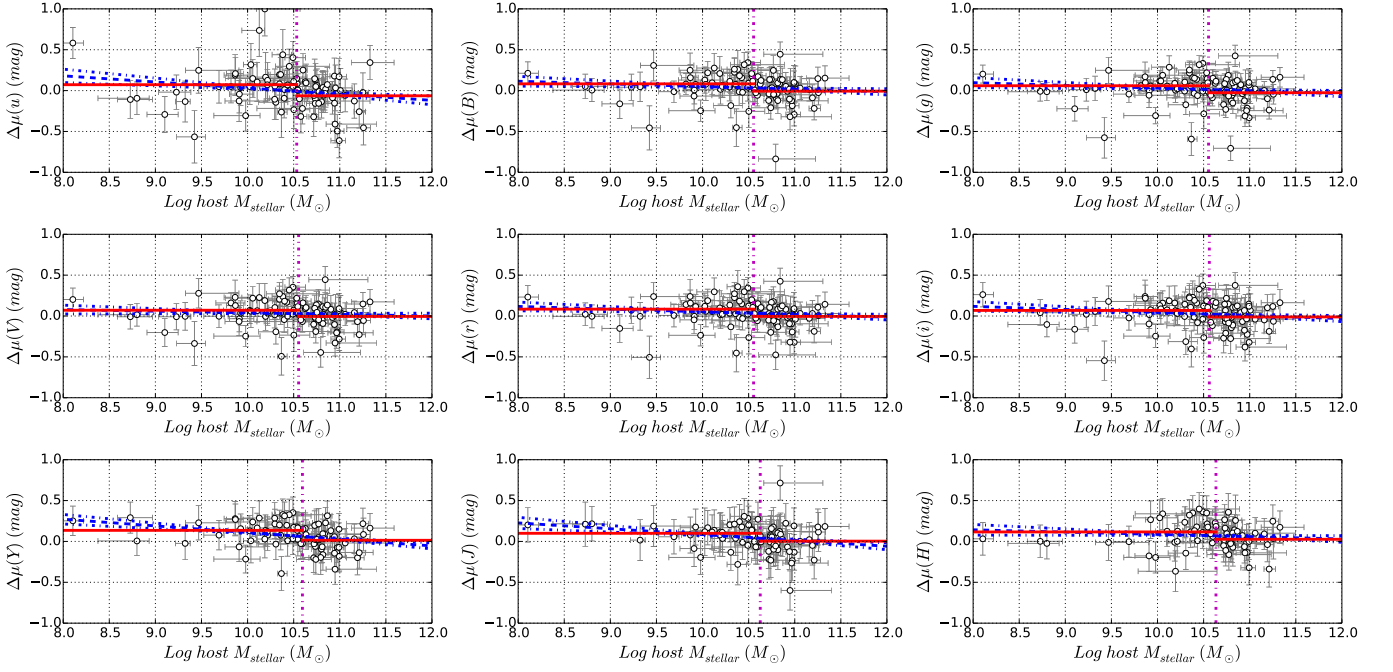


Figure 9. Same as Fig. 7 but including SNe Ia with $z > 0.01$.

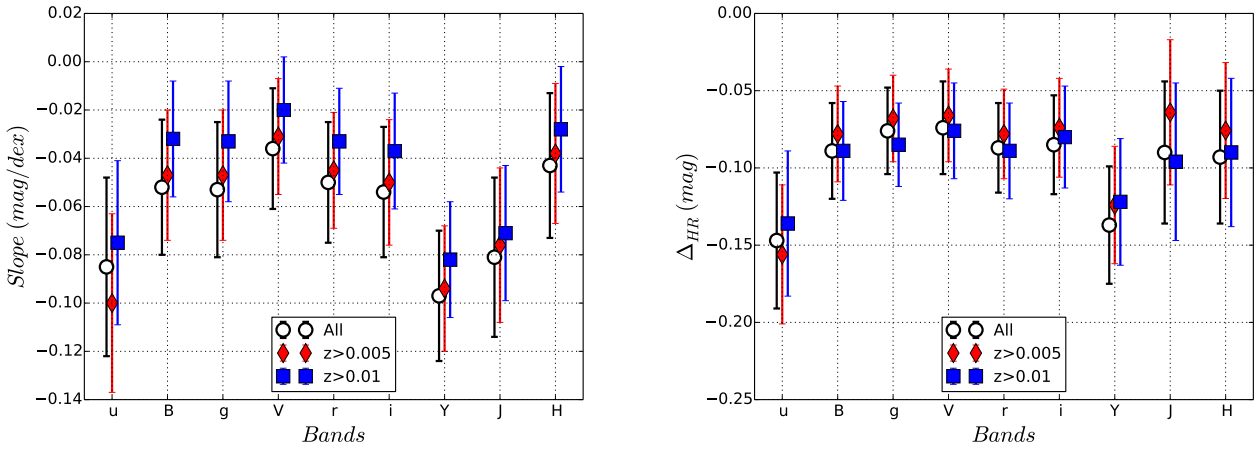


Figure 10. Variation of slope (left) and Δ_{HR} (right) in different bands. They are shown for the parent sample, $z > 0.005$ sample, and $z > 0.01$ sample. See Table 2 for the values of slopes and Δ_{HR} .

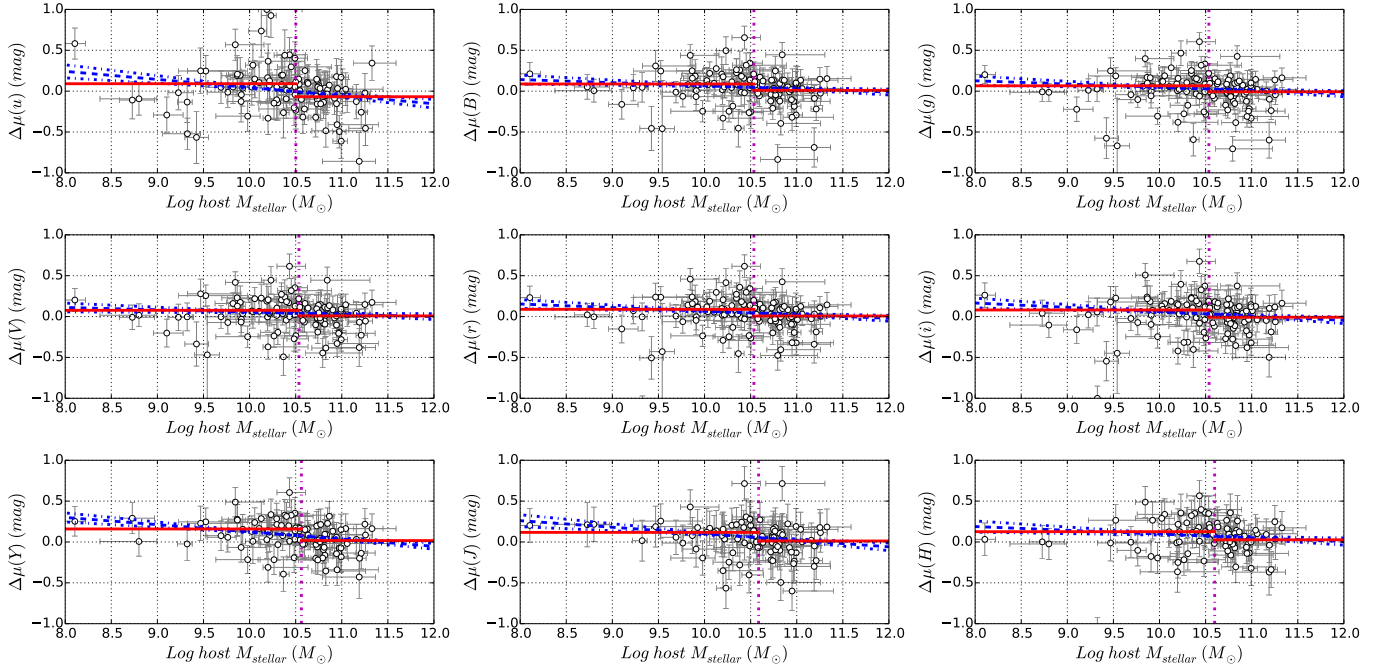


Figure 11. Same as Fig. 7 but including SNe Ia with $sBV > 0.5$ and $E(B - V) < 0.5$.

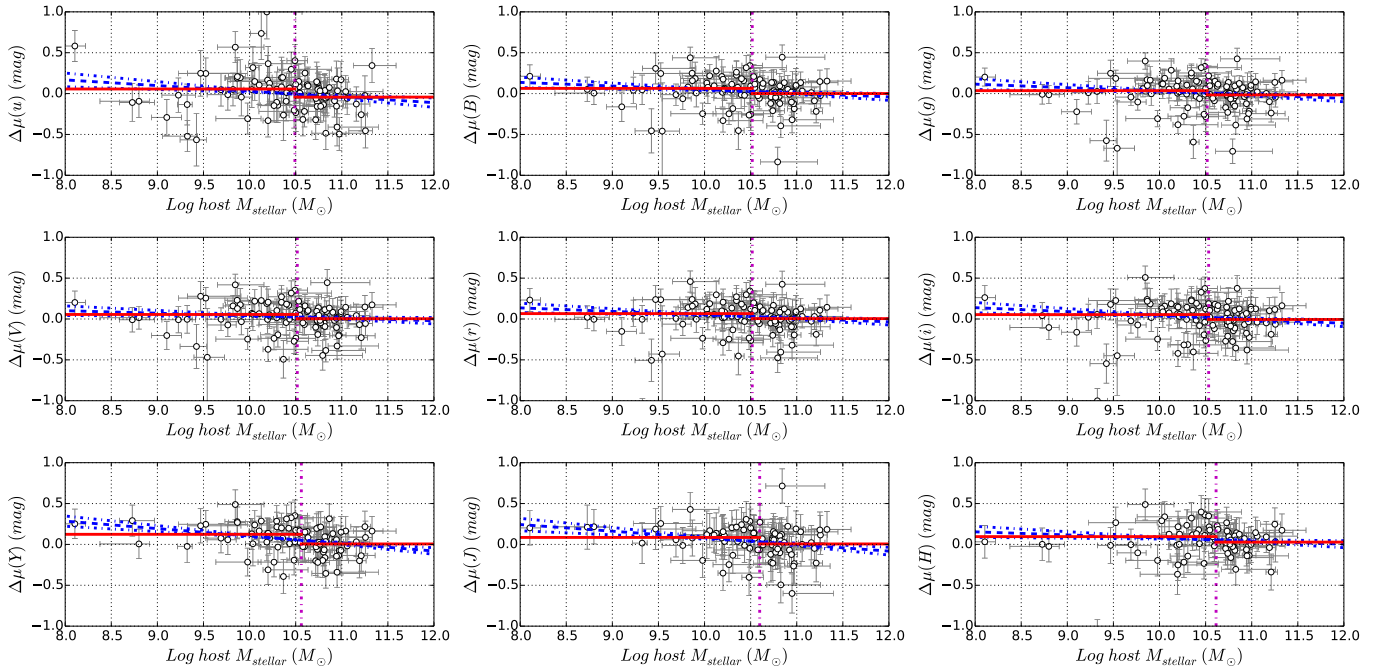


Figure 12. Same as Fig. 7 but excluding 91T- and 91bg-like SNe Ia.

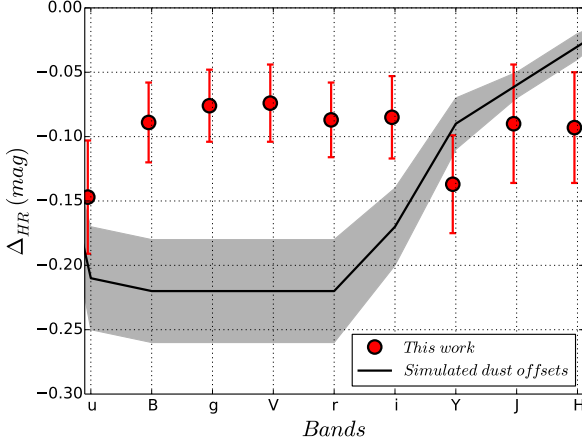


Figure 13. Similar to Fig. 10 (right) but adding simulated dust offsets according to Brout & Scolnic (2020). See subsection 4.2 for discussion.

3). For SNe Ia at redshifts $z > 0.005$ there is no appreciable change in their dispersions across the wavelengths compared to the full sample. But if we limit the sample to those at redshifts $z > 0.01$, an ~ 0.07 mag decrease in the dispersions for SNe Ia within 10 kpc is observed in all filters except u . Note, also, that the differences in the dispersions for the SNe beyond 10 kpc compared to those within 10 kpc grow smaller and tend to decrease with wavelength. This suggests that a combination of peculiar velocities and small errors in host dust corrections may be responsible for the observed difference in dispersion for SNe Ia within 10 kpc versus those beyond 10 kpc from the centers of their hosts.

Finally, looking at the host galaxy mass distribution, we find that for the inner sample (< 10 kpc), 75% of the hosts are massive ($\log M_{\text{stellar}}(M_{\odot}) > 10$), whereas for the outer sample (> 10 kpc), 88% of the hosts are massive. Hence, there is a small excess (13%) of massive host galaxies for SNe Ia that explode beyond 10 kpc from there host centers.

5. DISCUSSION

- (a) Our results on the correlation between SN Ia Hubble residual and host stellar mass are consistent with other published studies. When we compare our results with previous studies we find that results vary in magnitude (and significance) due to different sample size and analysis. Except for Burns et al. (2018), all previous studies used B -band Hubble residuals. Pan et al. (2014) studied the SN Ia Hubble residual-host mass correlation with a sample of 50 SNe Ia from the Palomar Transient Factory. They found a value of Δ_{HR} of

Table 2. Statistics on the SN Ia Hubble residual-host galaxy stellar mass correlation. Negative values in slopes indicate anti-correlation, i.e., SNe Ia are more luminous as host mass increases (see Fig. 7, 8, and 9). Errors in slopes and Δ_{HR} are in parentheses.

| Sample | Filter | Slope (mag dex ⁻¹) | Δ_{HR} (mag) |
|---|--------|-----------------------------------|------------------------|
| All | u | -0.085 (037) | -0.147 (044) |
| | B | -0.052 (028) | -0.089 (031) |
| | g | -0.053 (028) | -0.076 (028) |
| | V | -0.036 (025) | -0.074 (030) |
| | r | -0.050 (025) | -0.087 (029) |
| | i | -0.054 (027) | -0.085 (032) |
| | Y | -0.097 (027) | -0.137 (038) |
| | J | -0.081 (033) | -0.090 (046) |
| | H | -0.043 (030) | -0.093 (043) |
| $z > 0.005$ | u | -0.100 (037) | -0.156 (045) |
| | B | -0.047 (027) | -0.078 (031) |
| | g | -0.046 (027) | -0.068 (028) |
| | V | -0.031 (024) | -0.066 (030) |
| | r | -0.045 (024) | -0.078 (029) |
| | i | -0.050 (026) | -0.074 (032) |
| | Y | -0.093 (026) | -0.124 (038) |
| | J | -0.076 (032) | -0.064 (047) |
| | H | -0.038 (029) | -0.075 (044) |
| $z > 0.01$ | u | -0.075 (034) | -0.136 (047) |
| | B | -0.032 (024) | -0.089 (032) |
| | g | -0.033 (025) | -0.085 (027) |
| | V | -0.020 (022) | -0.076 (031) |
| | r | -0.033 (022) | -0.089 (031) |
| | i | -0.037 (024) | -0.080 (033) |
| | Y | -0.082 (024) | -0.122 (041) |
| | J | -0.071 (028) | -0.096 (051) |
| | H | -0.028 (026) | -0.090 (048) |
| $s_{BV} > 0.5$ & $E(B-V)_{\text{host}} < 0.5$ | u | -0.099 (033) | -0.166 (046) |
| | B | -0.038 (023) | -0.086 (031) |
| | g | -0.040 (023) | -0.083 (025) |
| | V | -0.028 (022) | -0.077 (031) |
| | r | -0.044 (022) | -0.090 (031) |
| | i | -0.053 (025) | -0.096 (033) |
| | Y | -0.088 (023) | -0.142 (042) |
| | J | -0.080 (030) | -0.103 (050) |
| | H | -0.046 (028) | -0.097 (047) |
| Exclude 91T– & 91bg–like SNe Ia | u | -0.070 (035) | -0.099 (045) |
| | B | -0.044 (026) | -0.063 (031) |
| | g | -0.043 (027) | -0.051 (028) |
| | V | -0.031 (024) | -0.052 (031) |
| | r | -0.043 (024) | -0.061 (030) |
| | i | -0.048 (026) | -0.060 (033) |
| | Y | -0.091 (026) | -0.118 (040) |
| | J | -0.081 (031) | -0.080 (049) |
| | H | -0.038 (028) | -0.067 (046) |

-0.08 ± 0.04 mag, and a slope of -0.041 ± 0.030 mag dex⁻¹. Childress et al. (2013a) used 115

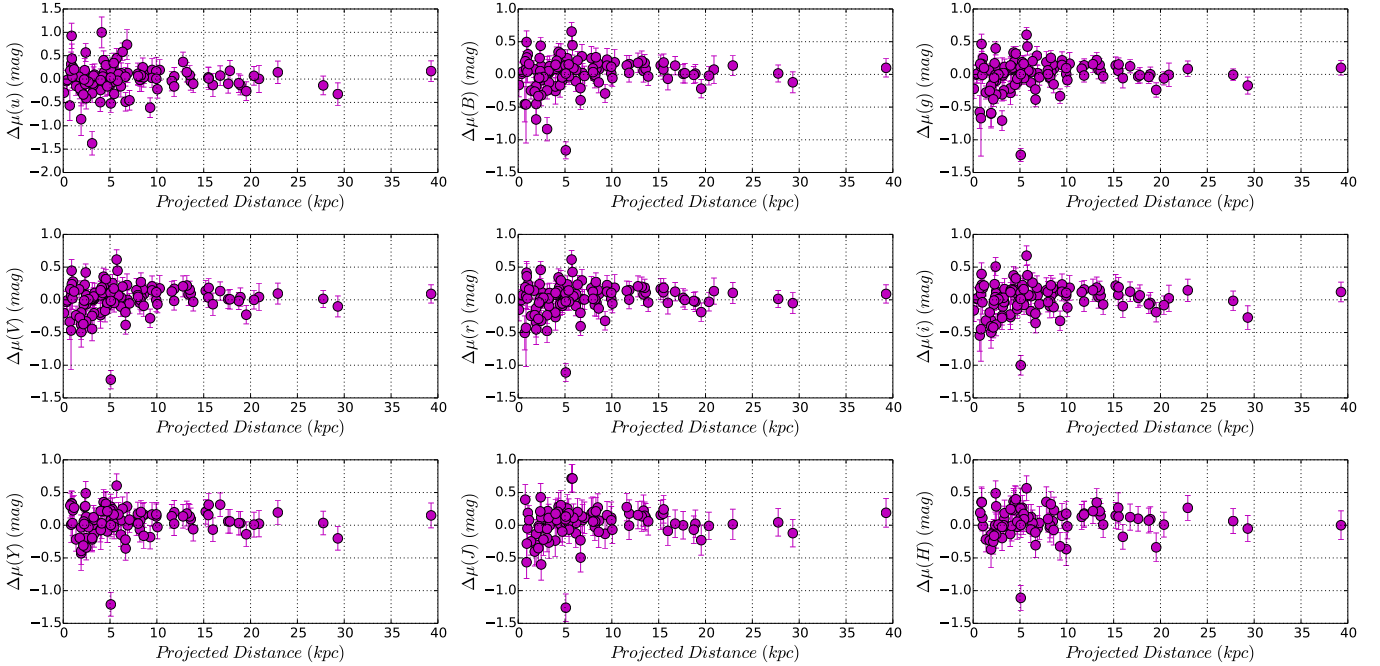


Figure 14. Variation of $\Delta\mu$ with projected distance from host centers in $uBgVriYJH$ bands. In all cases $\Delta\mu$ have smaller dispersion when they explode farther from their host centers.

SNe Ia from the Nearby Supernova Factory program and found a Δ_{HR} of -0.085 ± 0.028 mag, and a slope of -0.043 ± 0.014 mag dex $^{-1}$. Similar and consistent results were also presented from the SDSS (Lampeitl et al. 2010) and SNLS (Sullivan et al. 2010) samples. Uddin et al. (2017b) combined both spectroscopically confirmed and photometrically classified SNe Ia from multiple surveys and undertook a consistent analysis. They found a Δ_{HR} of -0.05 ± 0.01 mag from a sample of 1338 SNe Ia. In the CSP-I sample, we find similar correlations between Hubble residuals and host stellar mass across all wavelengths from optical to near-infrared, in apparent contradiction to the suggestion that dust explains the luminosity correction (Brout & Scolnic 2020).

- (b) Galbany et al. (2012) found a weak slope (-0.0019 ± 0.0022 mag kpc $^{-1}$) when studying the correlation between SN Ia Hubble residual and projected distance. The study presented in Hicken et al. (2009) is closer to this work, where they found 0.05 mag less dispersion in SNe Ia exploding beyond 12 kpc from their host centers.

Why do SNe Ia have a larger Hubble residuals when they explode closer to their hosts, while the dispersion gets smaller when they explode farther away? We suspect that dust in host galaxies may play a role here, particularly since the difference

in dispersion is largest at bluer wavelengths after eliminating the nearest SNe Ia. We examine this in Fig 15, where we encode $E(B - V)_{host}$ information in the plot of Hubble residual vs projected distance. We see that SNe Ia that explode beyond 10 kpc from host centers have a smaller variation in $E(B - V)_{host}$. On the other hand, SNe Ia that explode within 10 kpc of host centers have a large variation of $E(B - V)_{host}$. Moreover, it seems that SNe Ia with higher color excess are also more luminous after light-curve standardization (negative values of Hubble residuals).

In Fig. 16, we plot both $E(B - V)$ and the extinction law (R_V) with respect to the projected distance. One can see that SNe Ia that explode within 10 kpc of their host centers have large variations in color excess, whereas those that explode beyond 10 kpc of their host center have smaller variations in color excess. The extinction law seems not to vary according to separation.

- (c) Hicken et al. (2009) found that SNe Ia in spiral galaxies (Scd/Sd/Irr) are intrinsically fainter than their E/S0 counterparts, after light-curve correction. We have used galaxy morphological information in subsection 4.1, and use it again to examine how SN Ia Hubble residuals are distributed when they are grouped according to host morphological types. Contrary to Hicken et al. (2009), we do not

Table 3. Dispersion in Hubble residuals of SNe Ia that are within 10 kpc from their host centers and those that are beyond 10 kpc in various bands.

| Filter | Dispersion in $\Delta\mu$ (mag) | |
|------------------|---------------------------------|-----------------------------|
| | <i>Distance < 10 kpc</i> | <i>Distance > 10 kpc</i> |
| All | | |
| <i>u</i> | 0.34 | 0.16 |
| <i>B</i> | 0.27 | 0.10 |
| <i>g</i> | 0.27 | 0.11 |
| <i>V</i> | 0.25 | 0.10 |
| <i>r</i> | 0.25 | 0.10 |
| <i>i</i> | 0.25 | 0.12 |
| <i>Y</i> | 0.25 | 0.12 |
| <i>J</i> | 0.28 | 0.12 |
| <i>H</i> | 0.25 | 0.15 |
| <i>z</i> > 0.005 | | |
| <i>u</i> | 0.34 | 0.16 |
| <i>B</i> | 0.26 | 0.10 |
| <i>g</i> | 0.27 | 0.11 |
| <i>V</i> | 0.24 | 0.10 |
| <i>r</i> | 0.24 | 0.10 |
| <i>i</i> | 0.24 | 0.12 |
| <i>Y</i> | 0.25 | 0.12 |
| <i>J</i> | 0.27 | 0.12 |
| <i>H</i> | 0.24 | 0.15 |
| <i>z</i> > 0.01 | | |
| <i>u</i> | 0.31 | 0.14 |
| <i>B</i> | 0.20 | 0.10 |
| <i>g</i> | 0.20 | 0.11 |
| <i>V</i> | 0.18 | 0.10 |
| <i>r</i> | 0.18 | 0.10 |
| <i>i</i> | 0.18 | 0.12 |
| <i>Y</i> | 0.17 | 0.13 |
| <i>J</i> | 0.20 | 0.12 |
| <i>H</i> | 0.18 | 0.15 |

find a significant difference in the weighted means of $\Delta\mu(B)$ between spiral hosts and E/S0 hosts. We summarize the weighted means in Table 4. A recent study by (Pruzhinskaya et al. 2020) also supports our findings where they did not observe any difference in $\Delta\mu(B)$ between Early-type and Late-type SNe Ia host galaxies.

We note that galaxy morphology from NED is not homogeneous. The morphological classification method and images that are used to classify galaxies are also variable. A consistent classification scheme is therefore preferable. One such avenue will be a machine learning based galaxy morpho-

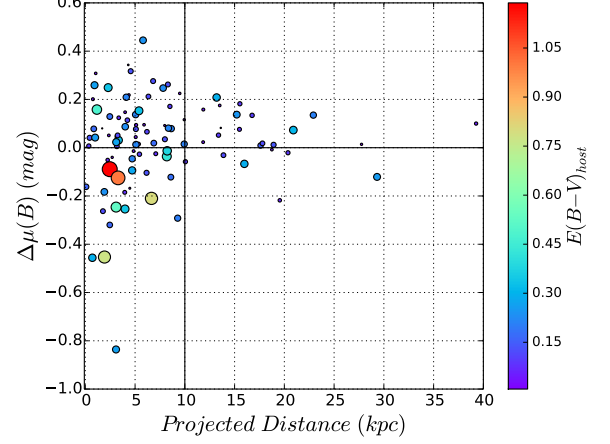


Figure 15. Plot of SN Ia Hubble residual against projected distances from host centers. Symbols in this dispersion plot are varying according to respective color excess values, $E(B - V)_{\text{host}}$. Redder and larger symbols refer to higher color excess. SNe Ia with larger color excess tend to reside closer to hosts and are more luminous.

logical analysis such as the one described in Barchi et al. (2020).

Table 4. Weighted mean of SN Ia Hubble residual in different host morphological types.

| Morphology | No. | Weighted mean of $\Delta\mu(B)$ (mag) |
|------------|-----|--|
| Spiral | 59 | 0.026 ± 0.051 |
| E | 9 | -0.038 ± 0.137 |
| S0 | 21 | 0.056 ± 0.087 |
| E + S0 | 30 | 0.028 ± 0.074 |

6. CONCLUSION

We have presented photometry of host galaxies of SNe Ia from the CSP-I in *ugriYJH* filters. We have determined host galaxy stellar masses, and have studied the correlation between host galaxy stellar mass and SNe Ia Hubble residual in the *uBgVriYJH* bands. We emphasize that this is the first time such a study has been made using optical and near-infrared Hubble residuals of SNe Ia. Our results are consistent with previous studies that SNe Ia are on average more luminous in massive hosts, after correcting for the luminosity-decline rate relation. Moreover, we find that the Hubble residual offset, Δ_{HR} , is approximately constant from optical to near-infrared wavelengths, suggesting that dust in SNe Ia host galaxies does not play a large role in driving these correlations. We have also determined projected distances be-

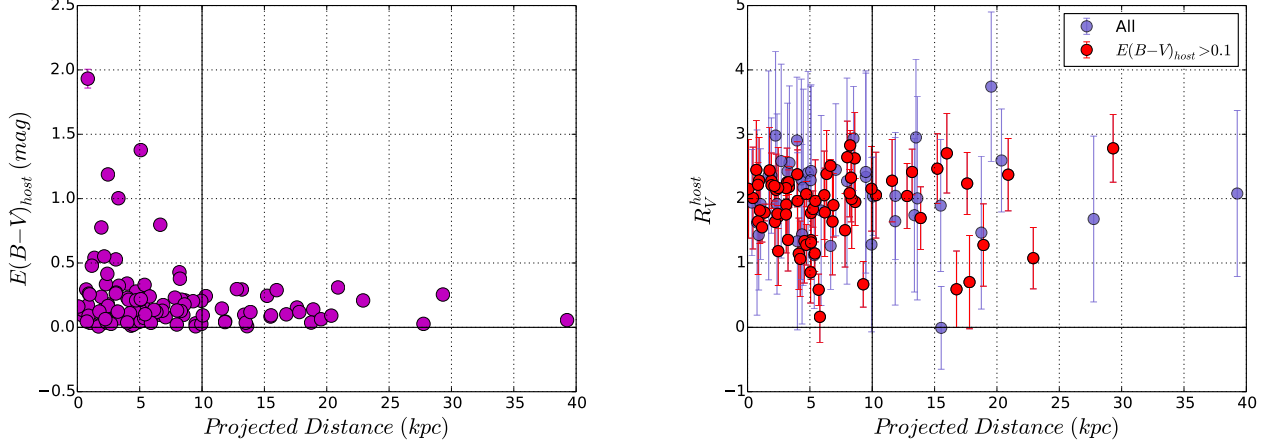


Figure 16. *Left:* Variation of color excess $E(B-V)_{\text{host}}$, and extinction law R_V^{host} , at the position of SN Ia as a function of the projected distance. The largest color excess is observed for SN 2008cd, which is within 5.5 arcsec from its host NGC 5038. SNe Ia exploding beyond 10kpc have $E(B-V)_{\text{host}} < 0.5$ mag. *Right:* Variation of extinction law R_V^{host} at the position of SNe Ia as a function of the projected distance. We do not observe significant variation of R_V .

tween the SNe and the centers of their host galaxies. We find that SNe Ia that explode beyond 10 kpc from their host galaxy centers have a smaller dispersion in their luminosities compared to those that explode within 10 kpc. These SNe also have a smaller variation in color excess than do SNe that explode within 10 kpc. SNe Ia exploding closer to host centers also more commonly have higher color excesses. These results should be confirmed with a larger sample with host galaxies clearly identified. We did not find differences in SN Ia standardized luminosities when they are grouped according to their host morphological types.

We are gathering integral-field spectroscopy of CSP SN Ia host galaxies (e.g., [Galbany et al. 2018](#)) to study their local environments. This may provide more insight into the origin of the observed luminosity offsets along with other findings.

ACKNOWLEDGMENTS

The work of the *Carnegie Supernova Project* has been supported by the National Science Foundation under grants AST0306969, AST0607438, AST1008343, AST1613426, AST1613472, and AST613455. NBS and KK gratefully acknowledge the support from the George P. and Cynthia Woods Mitchell Institute for Fundamental Physics and Astronomy. We also thank the Mitchell Foundation for their support of the Cooks Branch Workshop on Supernovae. M. S. is funded by generous grants from the Villum FONDEN and the Independent Research Fund Denmark. L.G. was funded by the European Union’s Horizon 2020 research and innovation program under the Marie Skłodowska-Curie grant agreement No. 839090. This work has been partially supported by the Spanish grant PGC2018-095317-B-C21 within the European Funds for Regional Development (FEDER).

APPENDIX

A. SN IA HUBBLE RESIDUAL

Table A1. CSP-I SN Ia Hubble Residuals

| <i>SN Name</i> | <i>u</i> | <i>B</i> | <i>g</i> | <i>V</i> | <i>r</i> | <i>i</i> | <i>Y</i> | <i>J</i> | <i>H</i> |
|----------------|-----------|-----------|-----------|-----------|-----------|-----------|-----------|-----------|-----------|
| 2004ef | 0.13(20) | 0.02(15) | 0.02(12) | -0.00(15) | 0.01(15) | 0.07(16) | -0.00(20) | 0.08(24) | -0.05(20) |
| 2004eo | -0.13(21) | 0.01(14) | 0.00(11) | 0.04(14) | -0.03(15) | -0.05(16) | 0.03(18) | 0.02(21) | 0.09(19) |
| 2004ey | 0.15(23) | 0.22(14) | 0.19(11) | 0.22(14) | 0.19(14) | 0.16(15) | 0.24(18) | 0.17(21) | 0.34(19) |
| 2004gs | 0.11(20) | 0.08(14) | 0.09(11) | 0.09(14) | 0.09(14) | 0.12(15) | 0.16(19) | 0.07(23) | 0.23(20) |
| 2004gu | 0.05(22) | 0.13(16) | 0.12(13) | 0.07(16) | 0.12(16) | 0.13(16) | 0.13(19) | 0.12(29) | 0.29(22) |
| 2005A | ... | -0.09(16) | -0.10(14) | -0.07(16) | 0.03(16) | 0.10(16) | -0.20(21) | -0.05(24) | -0.04(21) |
| 2005ag | ... | 0.05(17) | 0.07(14) | 0.08(17) | 0.08(17) | 0.04(17) | 0.13(20) | 0.22(24) | ... |
| 2005al | 0.40(20) | 0.34(13) | 0.33(09) | 0.35(13) | 0.34(13) | 0.37(14) | 0.35(19) | 0.28(22) | 0.36(20) |
| 2005am | -0.48(20) | -0.40(14) | -0.39(11) | -0.39(14) | -0.41(14) | -0.35(15) | -0.35(18) | -0.49(22) | -0.30(19) |
| 2005be | -0.09(24) | -0.01(17) | -0.03(14) | -0.04(16) | -0.01(15) | -0.01(16) | ... | ... | ... |
| 2005bg | -0.04(23) | 0.01(17) | -0.00(14) | -0.03(16) | -0.00(16) | 0.02(17) | ... | ... | ... |
| 2005bl | 0.00(27) | 0.08(22) | 0.04(20) | 0.04(21) | -0.04(22) | 0.07(20) | ... | ... | ... |
| 2005bo | -0.23(23) | -0.25(20) | -0.28(18) | -0.23(20) | -0.26(20) | -0.26(19) | ... | ... | ... |
| 2005el | -0.05(19) | 0.08(13) | 0.05(09) | 0.09(13) | 0.11(13) | 0.06(14) | 0.09(17) | 0.12(21) | 0.14(19) |
| 2005eq | -0.10(20) | 0.01(14) | -0.03(11) | 0.01(14) | 0.03(14) | 0.03(15) | 0.06(18) | -0.00(21) | 0.10(19) |
| 2005hc | 0.25(20) | 0.17(14) | 0.15(11) | 0.16(14) | 0.15(14) | 0.18(15) | 0.15(18) | 0.27(21) | 0.06(21) |
| 2005hj | -0.13(25) | 0.05(18) | 0.03(15) | -0.00(17) | -0.00(17) | 0.06(17) | -0.02(20) | 0.02(25) | ... |
| 2005iq | 0.09(20) | 0.17(13) | 0.14(10) | 0.15(13) | 0.18(13) | 0.14(14) | 0.14(18) | 0.14(21) | 0.21(19) |
| 2005ir | -0.02(21) | 0.04(16) | 0.01(14) | -0.01(16) | 0.07(16) | 0.02(16) | ... | ... | ... |
| 2005kc | -0.06(20) | 0.03(14) | 0.02(11) | 0.02(14) | 0.03(14) | -0.04(15) | -0.02(18) | 0.00(21) | 0.10(19) |
| 2005ke | 0.45(21) | 0.66(14) | 0.60(11) | 0.61(15) | 0.61(14) | 0.68(15) | 0.60(18) | 0.71(21) | 0.56(19) |
| 2005ki | -0.14(20) | 0.01(13) | -0.01(09) | 0.01(13) | 0.01(13) | -0.02(15) | 0.03(18) | 0.04(21) | 0.06(19) |
| 2005ku | 0.32(26) | 0.08(20) | 0.12(18) | 0.06(20) | 0.06(19) | 0.09(19) | 0.01(27) | ... | ... |
| 2005lu | 0.19(25) | 0.25(21) | 0.17(18) | 0.23(21) | 0.24(21) | 0.24(20) | 0.28(21) | ... | ... |
| 2005M | -0.09(20) | 0.01(14) | -0.01(11) | 0.02(14) | -0.00(14) | -0.10(15) | 0.01(18) | 0.22(21) | -0.02(19) |
| 2005mc | 0.03(28) | 0.02(25) | 0.02(23) | 0.02(24) | 0.01(23) | 0.04(22) | ... | ... | ... |
| 2005na | -0.49(20) | -0.18(14) | -0.21(11) | -0.20(14) | -0.20(14) | -0.23(15) | -0.07(18) | -0.23(24) | -0.14(19) |
| 2005W | 0.19(22) | 0.18(20) | 0.16(17) | 0.17(20) | 0.18(20) | 0.18(19) | ... | ... | ... |
| 2006ax | -0.09(20) | -0.01(13) | -0.04(10) | -0.02(13) | -0.02(13) | -0.07(14) | 0.03(18) | -0.07(21) | 0.07(19) |
| 2006bd | ... | 0.25(18) | 0.19(16) | 0.15(18) | 0.18(18) | 0.15(19) | 0.05(20) | 0.18(24) | 0.36(23) |
| 2006bh | 0.06(19) | 0.16(13) | 0.14(10) | 0.17(13) | 0.15(13) | 0.16(14) | 0.20(18) | 0.18(21) | 0.18(19) |
| 2006br | ... | -0.12(18) | -0.24(15) | -0.20(19) | -0.10(19) | -0.04(19) | -0.14(20) | -0.27(24) | -0.01(22) |
| 2006D | -0.01(19) | -0.06(13) | -0.10(10) | -0.07(14) | -0.06(14) | -0.07(15) | 0.06(18) | -0.01(22) | -0.10(19) |
| 2006mr | -0.86(35) | -0.69(24) | -0.60(22) | -0.38(23) | -0.34(23) | -0.50(24) | -0.43(26) | -0.30(30) | -0.37(28) |
| 2006ef | 0.20(25) | 0.23(17) | 0.21(13) | 0.20(16) | 0.23(15) | 0.23(16) | ... | ... | ... |
| 2006ej | 0.09(23) | 0.12(16) | 0.11(12) | 0.10(15) | 0.10(15) | 0.16(16) | 0.08(18) | -0.01(22) | 0.18(20) |
| 2006eq | 0.17(30) | 0.01(18) | 0.01(15) | -0.01(17) | 0.01(17) | 0.07(18) | 0.14(19) | 0.12(24) | -0.36(25) |
| 2006et | -0.04(19) | -0.09(13) | -0.12(10) | -0.08(13) | -0.09(13) | -0.14(14) | -0.09(17) | -0.04(21) | -0.02(19) |
| 2006ev | ... | 0.14(16) | 0.14(13) | 0.14(16) | 0.17(16) | 0.22(17) | 0.21(19) | 0.16(22) | 0.15(20) |

Table A1 continued

Table A1 (continued)

| <i>SN Name</i> | <i>u</i> | <i>B</i> | <i>g</i> | <i>V</i> | <i>r</i> | <i>i</i> | <i>Y</i> | <i>J</i> | <i>H</i> |
|----------------|-----------|-----------|-----------|-----------|-----------|-----------|-----------|-----------|-----------|
| 2006fw | -0.57(32) | -0.46(27) | -0.58(25) | -0.34(27) | -0.51(26) | -0.55(24) | ... | ... | ... |
| 2006gj | 0.15(21) | 0.21(15) | 0.22(12) | 0.22(15) | 0.20(15) | 0.19(16) | 0.18(19) | 0.14(23) | 0.35(21) |
| 2006gt | 0.04(22) | 0.08(15) | 0.06(12) | 0.04(15) | 0.12(15) | 0.08(16) | 0.16(18) | 0.18(22) | 0.27(23) |
| 2006hb | 0.13(22) | 0.07(15) | 0.04(11) | 0.04(15) | 0.09(15) | 0.06(16) | 0.08(19) | 0.04(22) | 0.13(19) |
| 2006hx | -0.14(21) | -0.18(15) | -0.17(12) | -0.19(15) | -0.13(15) | -0.31(16) | -0.03(19) | -0.13(22) | -0.14(20) |
| 2006is | -0.08(29) | -0.17(18) | -0.16(16) | -0.17(17) | -0.07(17) | 0.11(19) | 0.28(22) | 0.02(28) | 0.34(26) |
| 2006kf | 0.01(21) | 0.09(15) | 0.09(12) | 0.11(15) | 0.08(14) | 0.10(15) | 0.09(18) | 0.10(21) | 0.10(20) |
| 2006lu | -0.11(25) | 0.04(17) | -0.01(14) | 0.01(16) | 0.03(16) | -0.01(17) | 0.28(19) | ... | ... |
| 2006ob | -0.46(21) | -0.03(15) | -0.04(12) | -0.06(15) | 0.01(15) | -0.07(15) | 0.09(20) | 0.12(24) | 0.04(25) |
| 2006os | -0.02(25) | -0.04(17) | -0.06(14) | -0.05(17) | -0.08(17) | -0.10(18) | -0.07(19) | -0.03(21) | -0.04(22) |
| 2006py | -0.29(22) | -0.16(18) | -0.22(15) | -0.20(17) | -0.15(17) | -0.16(17) | ... | ... | ... |
| 2006X | -0.52(19) | -1.16(13) | -1.23(10) | -1.22(14) | -1.11(14) | -1.00(15) | -1.21(18) | -1.26(21) | -1.11(19) |
| 2007af | 0.25(19) | 0.25(13) | 0.19(10) | 0.26(13) | 0.24(13) | 0.23(14) | 0.25(17) | 0.26(21) | 0.27(19) |
| 2007ai | -0.13(25) | -0.07(17) | -0.06(15) | -0.07(17) | -0.05(17) | -0.10(17) | -0.07(18) | -0.09(22) | -0.18(19) |
| 2007al | 0.25(28) | 0.31(19) | 0.25(16) | 0.28(18) | 0.24(17) | 0.18(19) | 0.23(21) | 0.19(25) | -0.01(22) |
| 2007as | 0.20(21) | 0.08(14) | 0.06(11) | 0.04(14) | 0.03(14) | 0.11(15) | 0.08(18) | 0.04(21) | 0.12(19) |
| 2007ax | 0.93(27) | 0.49(17) | 0.47(15) | 0.45(17) | 0.41(17) | 0.40(17) | 0.34(19) | -0.56(25) | 0.35(23) |
| 2007ba | -0.61(21) | -0.29(14) | -0.33(11) | -0.28(14) | -0.32(14) | -0.32(15) | -0.18(18) | -0.13(22) | -0.32(21) |
| 2007bc | -0.10(19) | -0.03(14) | -0.03(10) | -0.03(14) | -0.04(14) | -0.07(15) | -0.06(18) | 0.06(21) | 0.01(20) |
| 2007bd | -0.06(21) | 0.01(13) | -0.03(10) | 0.01(14) | -0.01(14) | 0.01(15) | 0.04(18) | 0.04(22) | 0.06(20) |
| 2007bm | -0.15(20) | -0.25(13) | -0.28(10) | -0.24(14) | -0.25(14) | -0.32(15) | -0.22(18) | -0.25(21) | -0.22(19) |
| 2007ca | 0.05(20) | -0.01(13) | -0.04(10) | -0.00(14) | 0.01(14) | -0.02(15) | 0.08(18) | 0.06(21) | -0.00(19) |
| 2007cg | -0.26(31) | -0.45(23) | -0.59(20) | -0.49(23) | -0.45(23) | -0.40(22) | -0.39(21) | ... | ... |
| 2007hj | 0.30(21) | 0.32(15) | 0.32(11) | 0.32(15) | 0.30(15) | 0.33(16) | 0.33(19) | 0.31(22) | 0.40(20) |
| 2007hx | 0.00(29) | 0.07(21) | -0.01(18) | 0.04(21) | 0.13(20) | 0.02(20) | 0.02(20) | ... | ... |
| 2007jd | 0.74(32) | 0.28(18) | 0.29(14) | 0.23(17) | 0.30(17) | 0.19(18) | 0.29(21) | 0.14(25) | ... |
| 2007jg | 0.58(19) | 0.21(14) | 0.20(11) | 0.20(14) | 0.23(14) | 0.26(15) | 0.25(18) | 0.20(21) | 0.03(20) |
| 2007jh | ... | 0.09(22) | 0.07(20) | 0.07(21) | 0.08(21) | 0.15(20) | -0.07(30) | ... | ... |
| 2007le | 0.57(19) | 0.44(13) | 0.40(10) | 0.42(13) | 0.46(13) | 0.51(14) | 0.49(18) | 0.43(21) | 0.49(19) |
| 2007N | 1.00(33) | 0.21(21) | 0.09(18) | 0.19(21) | 0.10(21) | 0.16(21) | 0.03(23) | 0.08(26) | -0.01(23) |
| 2007nq | -0.26(20) | -0.22(14) | -0.24(11) | -0.23(14) | -0.19(14) | -0.19(15) | -0.14(19) | -0.23(23) | -0.34(22) |
| 2007ol | 0.05(20) | 0.08(13) | 0.06(10) | 0.16(13) | 0.14(13) | ... | ... | ... | ... |
| 2007on | 0.02(20) | 0.13(13) | 0.14(10) | 0.14(13) | 0.12(13) | 0.12(14) | 0.16(18) | 0.15(21) | 0.14(19) |
| 2007S | -0.31(19) | -0.25(13) | -0.31(10) | -0.25(13) | -0.24(13) | -0.25(14) | -0.22(17) | -0.20(21) | -0.20(19) |
| 2007st | -0.41(23) | -0.32(16) | -0.31(13) | -0.33(16) | -0.32(16) | -0.38(17) | -0.34(19) | -0.60(24) | -0.14(21) |
| 2007ux | 0.05(21) | 0.11(14) | 0.10(11) | 0.10(14) | 0.13(14) | 0.14(15) | 0.21(18) | 0.20(21) | 0.23(19) |
| 2008ar | 0.07(19) | 0.05(13) | 0.02(10) | 0.05(14) | 0.02(14) | 0.03(15) | 0.12(18) | 0.11(21) | 0.00(19) |
| 2008bc | 0.10(24) | 0.10(14) | 0.06(11) | 0.07(14) | 0.06(14) | 0.07(15) | 0.17(18) | 0.12(21) | 0.12(19) |
| 2008bi | 0.44(31) | 0.26(23) | 0.16(19) | 0.24(21) | 0.36(20) | 0.23(20) | 0.33(19) | -0.28(25) | 0.35(21) |
| 2008bq | 0.04(21) | -0.12(16) | -0.15(13) | -0.09(16) | -0.13(16) | -0.11(16) | -0.16(19) | -0.10(24) | -0.07(23) |
| 2008bt | 0.02(22) | 0.14(16) | 0.11(13) | 0.11(16) | 0.10(16) | 0.11(17) | 0.23(19) | 0.09(26) | 0.26(31) |

Table A1 continued

Table A1 (*continued*)

| <i>SN Name</i> | <i>u</i> | <i>B</i> | <i>g</i> | <i>V</i> | <i>r</i> | <i>i</i> | <i>Y</i> | <i>J</i> | <i>H</i> |
|----------------|-----------|-----------|-----------|-----------|-----------|-----------|-----------|-----------|-----------|
| 2008bz | 0.11(23) | 0.09(15) | 0.06(12) | 0.07(14) | 0.12(14) | 0.12(16) | 0.17(18) | 0.20(23) | ... |
| 2008C | 0.05(24) | 0.04(17) | -0.01(13) | 0.02(17) | 0.02(17) | -0.04(18) | 0.03(19) | -0.05(23) | 0.11(20) |
| 2008cc | -0.20(22) | -0.26(15) | -0.25(11) | -0.27(15) | -0.23(14) | -0.19(16) | -0.19(18) | -0.40(22) | -0.23(19) |
| 2008cd | ... | -0.46(59) | -0.67(58) | -0.47(60) | -0.43(59) | -0.45(49) | ... | ... | ... |
| 2008cf | -0.11(23) | 0.05(15) | -0.01(12) | -0.01(15) | 0.02(14) | 0.04(16) | 0.29(19) | 0.21(27) | 0.00(20) |
| 2008fl | -0.15(23) | -0.10(16) | -0.12(12) | -0.10(15) | -0.09(15) | -0.17(17) | -0.14(18) | -0.12(22) | -0.06(20) |
| 2008fp | -0.33(20) | -0.33(14) | -0.38(11) | -0.37(15) | -0.29(15) | -0.42(16) | -0.31(18) | -0.35(21) | -0.25(19) |
| 2008fr | 0.18(26) | 0.20(15) | 0.16(12) | 0.16(15) | 0.19(15) | 0.18(16) | 0.30(19) | 0.39(23) | 0.19(19) |
| 2008fu | -0.06(22) | -0.04(16) | -0.00(12) | 0.01(15) | 0.03(14) | 0.01(16) | -0.03(19) | -0.22(24) | 0.01(20) |
| 2008fw | -0.04(21) | 0.14(15) | 0.09(11) | 0.13(15) | 0.14(15) | 0.12(16) | 0.14(18) | 0.28(21) | 0.13(19) |
| 2008gg | 0.14(24) | 0.14(15) | 0.09(12) | 0.10(16) | 0.10(16) | 0.14(17) | 0.20(18) | 0.01(23) | 0.27(19) |
| 2008gl | 0.07(21) | 0.13(14) | 0.12(10) | 0.13(14) | 0.12(14) | 0.12(15) | 0.31(18) | 0.02(21) | 0.12(20) |
| 2008go | 0.18(22) | 0.02(15) | -0.01(12) | 0.01(15) | -0.00(15) | 0.07(16) | 0.06(18) | ... | ... |
| 2008gp | -0.16(22) | 0.02(14) | -0.02(10) | -0.02(14) | 0.00(14) | -0.03(15) | 0.02(18) | -0.01(21) | 0.16(20) |
| 2008hj | 0.01(24) | 0.18(13) | 0.15(10) | 0.18(14) | 0.18(14) | 0.19(15) | 0.31(17) | 0.24(21) | 0.13(20) |
| 2008hu | 0.17(22) | 0.10(14) | 0.10(11) | 0.09(14) | 0.09(14) | 0.12(15) | 0.15(19) | 0.19(22) | 0.00(22) |
| 2008hv | 0.01(20) | 0.12(13) | 0.10(09) | 0.12(13) | 0.11(13) | 0.11(14) | 0.17(18) | 0.08(21) | 0.18(19) |
| 2008ia | -0.01(21) | -0.05(15) | -0.05(12) | -0.01(15) | -0.04(15) | -0.01(15) | 0.02(18) | -0.04(21) | -0.16(19) |
| 2008O | 0.34(21) | 0.15(15) | 0.16(12) | 0.17(15) | 0.14(15) | 0.16(16) | 0.16(18) | 0.18(22) | 0.17(20) |
| 2008R | -0.02(24) | 0.15(14) | 0.14(11) | 0.15(14) | 0.11(14) | 0.12(15) | 0.22(19) | 0.18(22) | 0.25(20) |
| 2009aa | -0.22(19) | -0.06(13) | -0.09(10) | -0.07(13) | -0.06(14) | -0.12(14) | -0.03(18) | -0.07(21) | -0.02(19) |
| 2009ab | 0.08(20) | 0.26(14) | 0.25(11) | 0.27(14) | 0.27(14) | 0.22(15) | 0.20(18) | 0.21(21) | 0.32(19) |
| 2009ad | -0.32(20) | -0.03(13) | -0.06(10) | -0.05(14) | -0.03(14) | -0.08(15) | -0.03(18) | -0.07(21) | 0.09(19) |
| 2009ag | 0.37(21) | 0.18(15) | 0.16(13) | 0.21(16) | 0.21(16) | 0.15(17) | 0.14(18) | 0.16(21) | 0.22(19) |
| 2009al | -0.32(24) | -0.12(16) | -0.17(13) | -0.10(16) | -0.05(16) | -0.27(18) | -0.20(18) | -0.12(21) | -0.05(20) |
| 2009cz | 0.07(20) | 0.04(13) | 0.01(11) | 0.04(14) | 0.01(14) | -0.04(15) | 0.03(18) | 0.06(21) | 0.10(20) |
| 2009D | 0.07(20) | -0.02(14) | -0.06(10) | -0.00(14) | -0.03(14) | -0.08(14) | 0.01(19) | -0.01(21) | 0.01(19) |
| 2009ds | -0.16(20) | -0.05(14) | -0.07(10) | -0.05(14) | -0.06(14) | -0.09(15) | 0.21(19) | -0.10(21) | 0.05(19) |
| 2009F | -1.38(25) | -0.84(18) | -0.71(15) | -0.45(18) | -0.48(18) | -0.28(18) | -0.20(21) | -0.06(24) | -0.03(22) |
| 2009I | 0.05(20) | -0.21(14) | -0.23(10) | -0.19(14) | -0.20(14) | -0.21(15) | -0.22(18) | -0.23(21) | -0.11(19) |
| 2009le | -0.04(23) | 0.45(15) | 0.42(13) | 0.45(16) | 0.42(16) | 0.38(16) | ... | 0.71(21) | ... |
| 2009P | 0.21(20) | 0.16(16) | 0.10(13) | 0.13(16) | 0.16(16) | 0.22(16) | 0.27(19) | 0.08(22) | ... |
| 2009Y | 0.03(20) | 0.01(14) | 0.00(11) | -0.02(14) | -0.03(14) | 0.01(15) | 0.00(18) | 0.13(21) | 0.00(19) |

B. HOST GALAXY PHOTOMETRY

We include a table of $ugriYJH$ photometry of CSP-I SN Ia host galaxies. Values within parentheses are uncertainties of measurements. When photometry is not available, it is shown as \dots . Morphological classification are taken from the NED.

Table B1. CSP-I Host Galaxy Photometry

| <i>SN Name</i> | <i>Host Galaxy Name</i> | <i>Morphology</i> | <i>u</i> | <i>g</i> | <i>r</i> | <i>i</i> | <i>Y</i> | <i>J</i> | <i>H</i> |
|----------------|--------------------------------|-------------------|-----------|-----------|-----------|-----------|-----------|-----------|-----------|
| 2004ef | UGC 12158 | SA | 17.44(08) | 14.07(04) | 13.40(06) | 13.12(03) | 12.39(12) | 11.77(12) | 11.12(09) |
| 2004eo | NGC 6928 | SB | 14.64(08) | 12.68(05) | 11.83(08) | 11.09(13) | ... | 9.81(02) | 9.07(03) |
| 2004ey | UGC 11816 | SB | 18.02(08) | 13.90(06) | 13.44(11) | 13.18(11) | 12.08(05) | 12.23(06) | 11.54(08) |
| 2004gs | MCG +03-22-020 | S | 16.65(08) | 14.65(06) | 13.72(11) | 13.32(11) | 12.46(10) | 12.05(09) | 11.33(09) |
| 2004gu | FGC 175A | ... | 19.24(09) | 17.23(08) | 16.48(08) | 16.01(08) | 14.53(09) | 14.07(10) | 13.16(12) |
| 2005A | NGC 958 | SB | 14.29(09) | 12.49(11) | 11.85(09) | 11.41(12) | 10.49(12) | 9.91(14) | 9.03(16) |
| 2005ag | 2MASS J14564320+0919366 | ... | ... | 16.26(08) | 15.49(07) | 15.06(08) | 14.14(07) | 13.57(12) | 12.97(10) |
| 2005al | NGC 5304 | cD | 15.17(10) | 13.22(07) | 12.37(06) | 11.99(07) | 10.93(16) | 10.14(14) | 9.94(12) |
| 2005am | NGC 2811 | SB | 13.55(09) | 11.70(09) | 10.93(09) | 10.50(09) | 9.32(09) | 8.90(08) | 8.38(08) |
| 2005be | 2MASS J14593308+1640068 | ... | 17.67(07) | 15.45(11) | 14.51(11) | 14.16(06) | ... | 12.76(04) | 12.01(05) |
| 2005bg | MCG +03-31-93 | ... | 15.89(14) | 14.79(12) | 14.24(14) | 14.02(13) | ... | 12.96(04) | 12.33(06) |
| 2005bl | NGC 4059 | E | 15.55(14) | 13.48(11) | 12.68(09) | 12.20(06) | ... | 10.73(02) | 10.01(02) |
| 2005bo | NGC 4708 | SA | 16.03(07) | 13.79(10) | 13.10(10) | 12.40(04) | ... | 11.16(03) | 10.52(04) |
| 2005el | NGC 1819 | SO | 15.38(10) | 13.37(06) | 12.17(09) | 11.79(07) | 10.89(09) | 10.44(10) | 9.78(10) |
| 2005eq | MCG -01-09-006 | SB | 17.00(09) | 14.18(03) | 13.53(08) | 13.16(10) | 12.75(14) | 12.36(15) | 11.75(16) |
| 2005hc | MCG +00-06-003 | ... | 18.50(11) | 15.66(08) | 14.91(10) | 14.54(10) | 13.59(13) | 13.21(20) | 12.55(12) |
| 2005hj | APMUKS(BJ) B012415.21-012950.3 | ... | 20.05(12) | 18.99(02) | 18.26(01) | 17.88(02) | 16.81(10) | 16.24(11) | 15.43(28) |
| 2005iq | MCG -03-01-008 | SA | 17.76(09) | 15.01(08) | 14.29(09) | 13.94(08) | 13.08(12) | 12.60(18) | 12.07(19) |
| 2005ir | SDSS J011643.87+004736.9 | ... | 18.58(04) | 17.40(08) | 16.87(07) | 16.49(06) | ... | 15.77(14) | 15.01(19) |
| 2005kc | NGC 7311 | SA | 14.25(15) | 12.50(05) | 11.76(07) | 11.33(07) | 10.40(09) | 9.22(07) | 8.67(09) |
| 2005ke | NGC 1371 | SA | 14.85(13) | 11.74(05) | 10.84(09) | 10.43(03) | ... | 8.75(02) | 8.08(02) |
| 2005ki | NGC 3332 | SA | 15.33(07) | 13.37(07) | 12.53(02) | 12.11(01) | 11.15(11) | 10.61(17) | 10.07(10) |
| 2005ku | 2MASX J22594265-0000478 | ... | 17.76(14) | 16.41(09) | 15.87(06) | 15.66(09) | 14.72(11) | 14.31(10) | 13.82(11) |
| 2005lu | ESO 545-G038 | SO | 16.26(14) | 15.49(04) | 14.55(29) | 14.28(07) | ... | 13.19(04) | 12.44(06) |
| 2005M | NGC 2930 | SO | 15.20(20) | 14.32(08) | 14.02(14) | 13.98(12) | 13.45(14) | 14.45(15) | 12.37(12) |
| 2005mc | UGC 4414 | SB | 16.84(37) | 14.70(05) | 13.47(09) | 12.86(10) | ... | 11.55(02) | 10.80(03) |
| 2005na | UGC 3634 | SB | 16.14(07) | 13.87(04) | 12.93(04) | 12.53(06) | 11.71(12) | 11.23(15) | 10.47(14) |
| 2005W | NGC 691 | SA | 15.64(11) | 12.93(09) | 12.05(13) | 11.76(11) | ... | 9.68(02) | 8.99(02) |
| 2006ax | NGC 3663 | SA | 15.47(12) | 14.06(04) | 13.09(04) | 12.14(04) | 12.14(12) | 11.38(12) | 10.79(12) |
| 2006bd | UGC 6609 | E | 17.52(32) | 14.17(07) | 13.34(05) | 12.90(05) | 11.71(12) | 11.65(13) | 10.98(17) |
| 2006bh | NGC 7329 | SB | 15.56(16) | 12.32(04) | 11.68(06) | 11.31(04) | 10.88(07) | 10.37(12) | 9.86(07) |
| 2006br | NGC 5185 | S | 16.04(05) | 13.66(07) | 12.99(05) | 12.27(05) | 11.59(09) | 11.15(07) | 10.45(12) |
| 2006D | MCG -01-33-34 | SB | 15.64(10) | 13.67(06) | 13.08(05) | 12.80(06) | 12.09(08) | 11.67(12) | 10.98(11) |
| 2006dd | NGC 1316 | SO | 11.77(12) | 9.84(05) | 9.17(04) | 8.66(03) | 8.00(04) | 6.80(05) | 6.22(04) |
| 2006ef | NGC 809 | SO | 16.21(12) | 13.96(06) | 13.17(07) | 12.77(06) | ... | 11.41(02) | 10.72(02) |
| 2006ej | NGC 191A | SO | 16.55(22) | 14.26(08) | 13.42(06) | 12.95(06) | 11.92(09) | 11.38(06) | 10.72(08) |
| 2006eq | 2MASX J21283758+0113490 | ... | 18.82(05) | 17.33(07) | 16.52(07) | 16.07(07) | 14.54(09) | 14.23(09) | 13.67(09) |
| 2006et | NGC 232 | SB | 17.21(18) | 14.05(06) | 13.18(09) | 12.73(07) | 11.52(09) | 11.19(06) | 10.41(07) |

Table B1 continued

Table B1 (*continued*)

| <i>SN Name</i> | <i>Host Galaxy Name</i> | <i>Morphology</i> | <i>u</i> | <i>g</i> | <i>r</i> | <i>i</i> | <i>Y</i> | <i>J</i> | <i>H</i> |
|----------------|--------------------------------|-------------------|-----------|-----------|-----------|-----------|-----------|-----------|-----------|
| 2006ev | UGC 11758 | S0 | 17.17(13) | 14.35(02) | 13.53(02) | 13.10(03) | 11.92(08) | 11.37(06) | 10.71(09) |
| 2006fw | SDSS J014710.33-000848.7 | | 19.85(23) | 18.88(07) | 18.28(08) | 17.84(08) | ... | 16.68(12) | 16.04(15) |
| 2006gj | UGC 2650 | SA | 17.27(22) | 14.98(04) | 14.13(03) | 13.69(04) | 12.48(17) | 12.03(13) | 11.34(17) |
| 2006gt | 2MASX J00561810-0137327 | ... | 19.72(28) | 17.10(08) | 16.26(06) | 15.89(05) | 15.21(13) | 14.80(08) | 14.14(14) |
| 2006hb | MCG -04-12-34 | E | 16.47(08) | 14.06(06) | 13.08(03) | 12.70(03) | 11.94(08) | 11.84(07) | 11.47(08) |
| 2006hx | 2MASX J01135716+0022171 | S0 | 18.49(09) | 16.45(04) | 15.70(04) | 15.32(05) | 14.17(07) | 13.55(07) | 12.91(09) |
| 2006is | APMUKS(BJ) B051529.79-235009.8 | ... | ... | 19.25(14) | 19.02(06) | 18.98(07) | 18.74(04) | 19.73(05) | ... |
| 2006kf | UGC 2829 | S0 | 16.57(08) | 13.74(06) | 12.93(04) | 12.55(05) | 11.38(09) | 10.90(09) | 10.33(11) |
| 2006lu | 2MASX J09151727-2536001 | ... | 18.30(06) | 16.29(05) | 15.72(05) | 15.39(05) | 14.48(14) | 14.04(07) | 13.36(13) |
| 2006ob | UGC 1333 | SA | 17.11(04) | 15.18(07) | 14.29(07) | 13.86(07) | 12.59(12) | 11.93(11) | 11.57(22) |
| 2006os | UGC 2384 | S | 17.04(33) | 14.43(04) | 13.60(04) | 13.24(04) | 12.20(08) | 11.66(09) | 11.25(09) |
| 2006py | SDSS J224142.04-000812.9 | ... | 20.06(08) | 18.23(07) | 17.47(05) | 17.05(04) | ... | 16.16(10) | 15.50(12) |
| 2006X | NGC 4321 | SB | 12.00(05) | 11.00(05) | 10.00(05) | 9.90(05) | 10.60(37) | 9.76(12) | 9.10(14) |
| 2007af | NGC 5584 | SB | 14.92(03) | 13.77(07) | 13.11(07) | 12.72(07) | 11.74(10) | 11.59(12) | 11.07(10) |
| 2007ai | MCG -04-38-004 | SA | ... | 13.75(06) | 12.84(02) | 12.86(03) | 12.05(09) | 11.31(19) | 10.72(11) |
| 2007al | 2MASX J09591870-1928233 | ... | 17.95(09) | 16.11(12) | 15.03(05) | 14.58(04) | 13.59(11) | 13.16(13) | 12.62(07) |
| 2007as | ESO 18-G18 | SA | 16.17(13) | 13.61(13) | 13.18(04) | 12.86(12) | 12.10(08) | 11.62(09) | 11.08(08) |
| 2007ax | NGC 2577 | S0 | 15.32(11) | 12.79(04) | 11.96(04) | 11.53(04) | 10.62(16) | 10.01(11) | 9.39(15) |
| 2007ba | UGC 9798 | S0 | 17.13(10) | 14.13(07) | 13.51(08) | 13.06(07) | 12.20(14) | 11.85(15) | 11.22(08) |
| 2007bc | UGC 6332 | SB | 16.09(12) | 13.64(10) | 12.57(32) | 12.50(05) | 11.50(22) | 11.23(17) | 10.56(12) |
| 2007bd | UGC 4455 | SB | 19.25(06) | 14.41(06) | 13.71(06) | 13.35(07) | 12.30(08) | 11.80(08) | 11.07(07) |
| 2007bm | NGC 3672 | SA | 13.77(04) | 11.84(11) | 11.15(08) | 10.75(06) | 10.27(09) | 9.73(06) | 9.09(11) |
| 2007ca | MCG -02-34-61 | SA | 18.71(24) | 14.45(05) | 13.96(06) | 13.73(05) | 12.90(16) | 12.61(18) | 11.84(10) |
| 2007cg | ESO 508-G75 | SA | 17.28(09) | 15.39(02) | 14.65(02) | 14.22(02) | 13.23(07) | 12.73(09) | 12.06(10) |
| 2007hj | NGC 7461 | S0 | 16.41(11) | 13.97(08) | 13.11(05) | 12.63(07) | 11.57(02) | 11.05(02) | 10.52(02) |
| 2007hx | SDSS J020627.93-005353.0 | ... | 19.29(08) | 16.96(06) | 16.29(06) | 15.82(05) | 15.04(09) | 14.27(07) | 13.71(09) |
| 2007jd | SDSS J025953.65+010936.1 | ... | 18.75(13) | 17.35(07) | 16.77(08) | 16.48(06) | 15.61(16) | 15.18(18) | 14.20(16) |
| 2007jg | SDSS J032950.83+000316.0 | ... | 19.47(10) | 18.74(08) | 17.46(06) | 17.49(07) | 16.97(13) | 17.27(17) | 16.44(20) |
| 2007jh | CGCG 391-014 | E | 17.22(08) | 14.83(10) | 13.85(20) | 13.57(08) | 12.50(13) | 11.82(22) | 11.29(16) |
| 2007le | NGC 7721 | SA | 13.93(18) | 12.35(04) | 11.72(04) | 11.39(05) | 11.08(02) | 10.38(09) | 9.52(08) |
| 2007N | MCG -01-33-012 | SA | 17.09(08) | 14.03(09) | 13.30(05) | 12.96(07) | 11.98(10) | 11.42(10) | 10.89(10) |
| 2007nq | UGC 595 | S | 17.09(08) | 14.53(10) | 13.57(09) | 13.10(09) | 12.25(11) | 11.81(12) | 11.06(16) |
| 2007ol | 2MASX J01372378-0018422 | ... | 18.96(15) | 17.05(12) | 16.29(12) | 15.84(07) | ... | 14.62(13) | 13.73(15) |
| 2007on | NGC 1404 | E | 12.94(07) | 10.72(11) | 10.05(09) | 9.59(08) | 8.45(25) | 8.23(25) | 7.72(26) |
| 2007S | UGC 5378 | SA | 15.43(18) | 14.15(10) | 13.74(08) | 13.39(09) | 12.51(06) | 11.77(05) | 11.48(08) |
| 2007st | NGC 692 | SB | 14.62(07) | 12.84(08) | 12.14(13) | 11.84(07) | 11.06(09) | 10.71(11) | 9.90(20) |
| 2007ux | 2MASX J10091969+1459268 | ... | 17.50(16) | 15.76(05) | 14.99(13) | 14.59(16) | 13.58(11) | 13.09(15) | 12.23(31) |
| 2008ar | IC 3284 | SA | 17.05(16) | 15.29(08) | 14.64(11) | 14.25(12) | 13.14(24) | 12.79(21) | 12.33(23) |
| 2008bc | KK 1524 | ... | 16.18(06) | 14.18(07) | 13.16(11) | 13.02(11) | 12.43(14) | 12.20(13) | 11.20(15) |
| 2008bi | NGC 2618 | SA | 16.37(06) | 13.31(06) | 12.53(09) | 12.04(08) | 10.36(53) | 10.90(18) | 10.40(07) |
| 2008bq | ESO 308-G25 | Sa | 17.80(04) | 14.19(01) | 13.46(01) | 13.06(01) | 12.08(09) | 11.61(09) | 10.87(09) |

Table B1 *continued*

Table B1 (*continued*)

| <i>SN Name</i> | <i>Host Galaxy Name</i> | <i>Morphology</i> | <i>u</i> | <i>g</i> | <i>r</i> | <i>i</i> | <i>Y</i> | <i>J</i> | <i>H</i> |
|----------------|--------------------------|-------------------|-----------|-----------|-----------|-----------|-----------|-----------|-----------|
| 2008bt | NGC 3404 | SB | 15.43(09) | 13.35(08) | 12.46(08) | 11.97(07) | 10.76(09) | 10.32(09) | 9.67(09) |
| 2008bz | 2MASX J12385810+1107502 | ... | 19.70(22) | 16.55(06) | 15.79(08) | 15.34(09) | 14.39(10) | 13.93(14) | 12.98(25) |
| 2008C | UGC 3611 | S0 | 16.33(14) | 14.06(07) | 13.31(09) | 12.88(09) | 11.96(12) | 11.21(13) | 10.58(13) |
| 2008cc | ESO 107-G4 | E | 14.89(05) | 12.79(06) | 12.01(09) | 11.62(08) | 10.57(12) | 10.15(17) | 9.49(17) |
| 2008cd | NGC 5038 | S0 | 14.32(11) | 12.78(03) | 12.15(06) | 11.81(05) | ... | 10.54(02) | 9.83(01) |
| 2008cf | LEDA 766647 | ... | 19.09(07) | 17.24(09) | 16.64(07) | 16.42(06) | 16.87(20) | 15.78(18) | 15.37(20) |
| 2008fl | NGC 6805 | E | 15.44(08) | 13.26(02) | 12.41(03) | 11.97(04) | 11.08(04) | 10.59(08) | 9.92(12) |
| 2008fp | ESO 428-G14 | S0 | 14.04(07) | 12.42(06) | 11.65(08) | 11.05(06) | 10.36(06) | 9.83(07) | 9.27(06) |
| 2008fr | SDSS J011149.19+143826.5 | ... | 20.83(14) | 19.44(07) | 18.77(11) | 18.58(10) | 18.72(15) | 18.07(11) | 17.76(12) |
| 2008fu | ESO 480-IG-021 | ... | 17.83(08) | 15.57(09) | 14.86(12) | 14.49(11) | 13.57(12) | 13.07(11) | 12.45(09) |
| 2008fw | NGC 3261 | SB | 14.85(04) | 12.66(09) | 12.03(09) | 11.41(10) | 10.41(17) | 10.03(16) | 9.34(21) |
| 2008gg | NGC 539 | SB | 16.48(06) | 14.34(05) | 13.53(15) | 13.24(12) | 12.59(09) | 11.91(08) | 11.51(08) |
| 2008gl | UGC 881 | E | 16.78(18) | 14.51(07) | 13.68(12) | 13.22(08) | 12.35(15) | 11.93(12) | 11.19(24) |
| 2008go | 2MASX J22104396-2047256 | ... | 18.08(10) | 15.94(05) | 14.98(07) | 14.41(07) | 13.72(14) | 12.91(40) | 11.68(64) |
| 2008gp | MCG +00-9-74 | SA | 16.25(12) | 14.20(09) | 13.61(09) | 13.26(08) | 12.55(09) | 12.03(11) | 11.26(23) |
| 2008hj | MCG -02-01-014 | SB | 16.76(03) | 15.08(10) | 14.37(05) | 14.14(06) | 13.84(08) | 13.36(18) | 12.52(11) |
| 2008hu | ESO 561-G18 | SA | 17.77(07) | 15.07(03) | 14.06(03) | 13.69(05) | 13.06(06) | 12.56(06) | 11.49(07) |
| 2008hv | NGC 2765 | S0 | 14.83(01) | 13.05(02) | 12.28(02) | 11.88(02) | 10.79(07) | 10.18(24) | 9.70(11) |
| 2008ia | ESO 125-6 | S0 | 15.58(04) | 13.17(11) | 12.38(13) | 12.02(13) | 11.64(06) | 10.86(16) | 10.35(08) |
| 2008O | ESO 256-G11 | S0 | 16.10(06) | 13.56(04) | 12.79(03) | 12.36(03) | 11.19(02) | 10.53(05) | 9.85(05) |
| 2008R | NGC 1200 | S0 | 15.38(13) | 13.04(28) | 11.90(11) | 11.41(10) | 10.71(16) | 10.23(20) | 9.56(11) |
| 2009aa | ESO 570-G20 | Sc | 19.91(14) | 15.02(07) | 14.42(00) | 13.67(03) | 13.15(09) | 12.47(16) | 12.04(17) |
| 2009ab | UGC 2998 | SB | 16.90(16) | 12.76(11) | 12.22(13) | 11.89(12) | 11.25(18) | 10.75(30) | 10.01(44) |
| 2009ad | UGC 3236 | SA | 16.97(10) | 14.68(09) | 13.98(11) | 13.43(14) | 12.69(08) | 12.25(15) | 11.61(10) |
| 2009ag | ESO 492-2 | SA | 16.75(04) | 12.02(11) | 11.62(11) | 11.37(12) | 11.01(08) | 10.52(08) | 9.90(10) |
| 2009al | NGC 3388 | S0 | 16.14(03) | 14.07(06) | 13.35(07) | 12.82(05) | 11.81(07) | 11.31(06) | 10.64(09) |
| 2009cz | NGC 2789 | S0 | 15.01(16) | 13.22(07) | 12.61(07) | 12.19(08) | 11.56(17) | 11.05(13) | 10.36(15) |
| 2009D | ESO 549-G031 | SA | 18.93(53) | 14.31(14) | 13.66(13) | 13.32(12) | 12.51(09) | 12.01(11) | 11.40(09) |
| 2009ds | NGC 3905 | SB | 14.57(08) | 13.37(10) | 12.22(08) | 11.15(12) | 11.76(13) | 10.99(13) | 10.45(12) |
| 2009F | NGC 1725 | ... | 15.57(12) | 13.23(08) | 12.37(07) | 11.67(11) | 9.90(20) | 9.96(25) | 9.37(22) |
| 2009I | NGC 1080 | SA | 15.26(07) | 13.75(08) | 12.93(06) | 12.23(07) | 12.09(08) | 11.62(06) | 11.10(08) |
| 2009le | ESO 478-6 | SA | 13.99(08) | 12.63(24) | 12.08(06) | 11.88(08) | 10.96(22) | 10.59(11) | 9.99(10) |
| 2009P | PGC 34730 | SB | 16.10(21) | 15.08(09) | 14.68(07) | 14.43(10) | 13.71(16) | 13.48(14) | 12.73(14) |
| 2009Y | NGC 5728 | SB | 14.21(05) | 11.85(10) | 11.21(10) | 10.84(09) | ... | 9.18(02) | 8.48(02) |

C. CSP-I HOST GALAXY PROPERTIES

We include host galaxy stellar mass of CSP-I SNe Ia as obtained using Z-PEG. Best-fit stellar mass are listed under M_{best} . Lower and upper limits of stellar masses are listed under M_{low} and M_{best} , respectively. We also include projected distance.

Table C1. Host Galaxy Properties

| <i>SN Name</i> | M_{low} | M_{best} | M_{high} | <i>Projected distance</i> |
|--------------------------------|-----------|------------|------------|---------------------------|
| $\log M_{stellar} (M_{\odot})$ | | | | (kpc) |
| 2004ef | 10.63 | 10.74 | 10.80 | 6.88 |
| 2004eo | 10.97 | 11.16 | 11.29 | 18.92 |
| 2004ey | 9.76 | 10.06 | 10.41 | 4.37 |
| 2004gs | 10.57 | 10.63 | 10.70 | 8.64 |
| 2004gu | 9.74 | 10.02 | 10.19 | 2.46 |
| 2005A | 11.07 | 11.19 | 11.26 | 2.45 |
| 2005ag | 10.84 | 10.90 | 10.95 | 13.38 |
| 2005al | 10.40 | 10.49 | 10.63 | 4.32 |
| 2005am | 10.68 | 10.83 | 11.26 | 6.67 |
| 2005be | 10.22 | 10.40 | 10.53 | 4.85 |
| 2005bg | 9.77 | 9.91 | 10.09 | 0.35 |
| 2005bl | 10.81 | 11.01 | 11.20 | 8.35 |
| 2005bo | 10.30 | 10.50 | 10.61 | 3.99 |
| 2005el | 10.70 | 10.84 | 11.24 | 13.61 |
| 2005eq | 10.40 | 10.56 | 10.65 | 17.61 |
| 2005hc | 10.52 | 10.60 | 10.65 | 8.50 |
| 2005hj | 9.22 | 9.32 | 9.38 | 3.21 |
| 2005iq | 10.47 | 10.54 | 10.60 | 13.51 |
| 2005ir | 9.07 | 9.23 | 9.43 | 0.43 |
| 2005kc | 10.60 | 11.06 | 11.50 | 3.33 |
| 2005ke | 10.30 | 10.43 | 10.62 | 5.71 |
| 2005ki | 10.62 | 10.80 | 10.86 | 27.76 |
| 2005ku | 9.96 | 10.04 | 10.10 | 0.85 |
| 2005lu | 9.70 | 9.86 | 9.99 | 2.29 |
| 2005M | 8.38 | 8.80 | 8.99 | 3.17 |
| 2005mc | 10.80 | 10.95 | 11.13 | 3.11 |
| 2005na | 10.90 | 10.97 | 11.05 | 3.96 |
| 2005W | 9.73 | 9.90 | 10.00 | 10.30 |
| 2006ax | 10.76 | 10.92 | 11.04 | 18.75 |
| 2006bd | 10.60 | 10.77 | 10.80 | 7.82 |
| 2006bh | 10.31 | 10.43 | 10.49 | 11.86 |
| 2006br | 10.87 | 10.97 | 11.36 | 3.29 |
| 2006D | 9.54 | 9.76 | 9.85 | 2.20 |
| 2006mr | 10.79 | 11.19 | 11.31 | 1.91 |
| 2006ef | 10.23 | 10.35 | 10.50 | 9.49 |
| 2006ej | 10.48 | 10.63 | 10.70 | 3.36 |
| 2006eq | 9.79 | 10.19 | 10.65 | 9.94 |

Table C1 *continued*

Table C1 (*continued*)

| <i>SN Name</i> | M_{low} | M_{best} | M_{high} | <i>Projected distance</i> (<i>kpc</i>) |
|----------------|--------------------------------|------------|------------|---|
| | $\log M_{stellar} (M_{\odot})$ | | | |
| 2006et | 10.70 | 10.80 | 10.88 | 4.71 |
| 2006ev | 10.65 | 10.75 | 10.91 | 15.22 |
| 2006fw | 9.26 | 9.42 | 9.61 | 0.71 |
| 2006gj | 10.36 | 10.53 | 10.60 | 13.19 |
| 2006gt | 9.87 | 9.93 | 9.94 | 15.49 |
| 2006hb | 10.04 | 10.22 | 10.38 | 6.19 |
| 2006hx | 10.12 | 10.31 | 10.44 | 1.91 |
| 2006is | 6.68 | 7.10 | 7.41 | 4.47 |
| 2006kf | 10.59 | 10.82 | 10.90 | 5.10 |
| 2006lu | 10.22 | 10.29 | 10.37 | 5.06 |
| 2006ob | 11.08 | 11.26 | 11.33 | 7.08 |
| 2006os | 10.66 | 10.81 | 10.87 | 8.19 |
| 2006py | 8.91 | 9.10 | 9.20 | 0.08 |
| 2006X | 9.06 | 9.33 | 9.51 | 5.09 |
| 2007af | 9.23 | 9.52 | 9.98 | 5.25 |
| 2007ai | 9.76 | 9.91 | 10.18 | 15.98 |
| 2007al | 9.33 | 9.47 | 9.91 | 1.05 |
| 2007as | 10.24 | 10.36 | 10.43 | 5.08 |
| 2007ax | 10.13 | 10.23 | 10.29 | 0.90 |
| 2007ba | 10.90 | 10.99 | 11.06 | 9.28 |
| 2007bc | 10.65 | 10.73 | 10.78 | 13.88 |
| 2007bd | 10.68 | 10.82 | 10.89 | 5.35 |
| 2007bm | 10.09 | 10.27 | 10.72 | 1.37 |
| 2007ca | 9.52 | 9.69 | 9.74 | 8.23 |
| 2007eg | 10.33 | 10.37 | 10.43 | 1.92 |
| 2007hj | 10.30 | 10.45 | 10.89 | 4.56 |
| 2007hx | 10.45 | 10.55 | 10.62 | 20.90 |
| 2007jd | 9.93 | 10.13 | 10.18 | 6.81 |
| 2007jg | 7.95 | 8.10 | 8.22 | 6.34 |
| 2007jh | 10.89 | 10.99 | 11.04 | 4.01 |
| 2007le | 9.71 | 9.85 | 10.16 | 2.40 |
| 2007N | 10.10 | 10.19 | 10.57 | 4.11 |
| 2007nq | 11.15 | 11.21 | 11.28 | 19.54 |
| 2007ol | 9.68 | 9.82 | 10.02 | 1.70 |
| 2007on | 10.78 | 11.04 | 11.45 | 9.49 |
| 2007S | 9.63 | 9.98 | 10.16 | 3.09 |
| 2007st | 10.85 | 10.95 | 11.40 | 2.46 |
| 2007ux | 10.23 | 10.30 | 10.34 | 4.23 |
| 2008ar | 10.11 | 10.21 | 10.28 | 3.25 |

Table C1 (*continued*)

Table C1 (*continued*)

| <i>SN Name</i> | M_{low} | M_{best} | M_{high} | <i>Projected distance</i> (kpc) |
|----------------|--------------------------------|------------|------------|------------------------------------|
| | $\log M_{stellar} (M_{\odot})$ | | | |
| 2008bc | 10.00 | 10.10 | 10.21 | 5.90 |
| 2008bi | 10.27 | 10.38 | 10.48 | 0.93 |
| 2008bq | 10.74 | 10.82 | 10.91 | 8.59 |
| 2008bt | 10.70 | 10.85 | 10.91 | 5.06 |
| 2008bz | 10.44 | 10.50 | 10.56 | 7.98 |
| 2008C | 10.35 | 10.49 | 10.55 | 0.99 |
| 2008cc | 10.40 | 10.48 | 10.64 | 1.77 |
| 2008cd | 9.37 | 9.54 | 9.67 | 0.84 |
| 2008cf | 8.59 | 8.73 | 8.97 | 2.36 |
| 2008ff | 10.87 | 10.94 | 11.01 | 6.15 |
| 2008fp | 10.15 | 10.20 | 10.63 | 2.15 |
| 2008fr | 7.58 | 7.73 | 7.89 | 0.76 |
| 2008fu | 10.66 | 10.72 | 10.80 | 2.70 |
| 2008fw | 10.31 | 10.49 | 10.61 | 11.59 |
| 2008gg | 10.63 | 10.73 | 10.82 | 22.91 |
| 2008gl | 10.81 | 10.86 | 10.92 | 16.76 |
| 2008go | 10.89 | 10.94 | 11.00 | 17.80 |
| 2008gp | 10.64 | 10.73 | 10.79 | 11.84 |
| 2008hj | 10.22 | 10.40 | 10.69 | 15.53 |
| 2008hu | 10.84 | 10.99 | 11.07 | 39.27 |
| 2008hv | 10.29 | 10.55 | 10.67 | 9.94 |
| 2008ia | 10.54 | 10.77 | 11.23 | 2.24 |
| 2008O | 11.12 | 11.33 | 11.59 | 5.39 |
| 2008R | 11.15 | 11.25 | 11.31 | 4.00 |
| 2009aa | 10.10 | 10.60 | 10.80 | 10.06 |
| 2009ab | 10.20 | 10.35 | 10.78 | 8.30 |
| 2009ad | 10.50 | 10.58 | 10.64 | 5.44 |
| 2009ag | 9.99 | 10.20 | 10.60 | 12.79 |
| 2009al | 10.66 | 10.72 | 10.77 | 29.32 |
| 2009cz | 10.68 | 10.75 | 10.84 | 8.00 |
| 2009D | 10.35 | 10.43 | 10.50 | 20.36 |
| 2009ds | 10.59 | 10.77 | 10.91 | 4.71 |
| 2009F | 10.61 | 10.79 | 11.22 | 3.08 |
| 2009I | 10.53 | 10.74 | 10.85 | 6.65 |
| 2009le | 10.66 | 10.84 | 11.31 | 5.80 |
| 2009P | 9.77 | 9.87 | 9.95 | 1.16 |
| 2009Y | 10.61 | 10.76 | 10.87 | 5.09 |

REFERENCES

- Barchi, P. H., de Carvalho, R. R., Rosa, R. R., et al. 2020, *Astronomy and Computing*, 30, 100334, doi: [10.1016/j.ascom.2019.100334](https://doi.org/10.1016/j.ascom.2019.100334)
- Bertin, E., & Arnouts, S. 1996, *A&AS*, 117, 393, doi: [10.1051/aas:1996164](https://doi.org/10.1051/aas:1996164)
- Betoule, M., Kessler, R., Guy, J., et al. 2014, *A&A*, 568, A22, doi: [10.1051/0004-6361/201423413](https://doi.org/10.1051/0004-6361/201423413)
- Blondin, S., & Tonry, J. L. 2007, *ApJ*, 666, 1024, doi: [10.1086/520494](https://doi.org/10.1086/520494)
- Brout, D., & Scolnic, D. 2020, arXiv e-prints, arXiv:2004.10206. <https://arxiv.org/abs/2004.10206>
- Burns, C. R., Stritzinger, M., Phillips, M. M., et al. 2011, *AJ*, 141, 19, doi: [10.1088/0004-6256/141/1/19](https://doi.org/10.1088/0004-6256/141/1/19)
- . 2014, *ApJ*, 789, 32, doi: [10.1088/0004-637X/789/1/32](https://doi.org/10.1088/0004-637X/789/1/32)
- Burns, C. R., Parent, E., Phillips, M. M., et al. 2018, *ApJ*, 869, 56, doi: [10.3847/1538-4357/aae51c](https://doi.org/10.3847/1538-4357/aae51c)
- Childress, M., Aldering, G., Antilogus, P., et al. 2013a, *ApJ*, 770, 108, doi: [10.1088/0004-637X/770/2/108](https://doi.org/10.1088/0004-637X/770/2/108)
- . 2013b, *ApJ*, 770, 107, doi: [10.1088/0004-637X/770/2/107](https://doi.org/10.1088/0004-637X/770/2/107)
- Contreras, C., Hamuy, M., Phillips, M. M., et al. 2010, *AJ*, 139, 519, doi: [10.1088/0004-6256/139/2/519](https://doi.org/10.1088/0004-6256/139/2/519)
- Fioc, M., & Rocca-Volmerange, B. 1997, *A&A*, 326, 950
- Folatelli, G., Morrell, N., Phillips, M. M., et al. 2013, *ApJ*, 773, 53, doi: [10.1088/0004-637X/773/1/53](https://doi.org/10.1088/0004-637X/773/1/53)
- Galbany, L., Miquel, R., Östman, L., et al. 2012, *ApJ*, 755, 125, doi: [10.1088/0004-637X/755/2/125](https://doi.org/10.1088/0004-637X/755/2/125)
- Galbany, L., Anderson, J. P., Sánchez, S. F., et al. 2018, *ApJ*, 855, 107, doi: [10.3847/1538-4357/aaaf20](https://doi.org/10.3847/1538-4357/aaaf20)
- Hamuy, M., Phillips, M. M., Maza, J., et al. 1995, *AJ*, 109, 1, doi: [10.1086/117251](https://doi.org/10.1086/117251)
- Hamuy, M., Trager, S. C., Pinto, P. A., et al. 2000, *AJ*, 120, 1479, doi: [10.1086/301527](https://doi.org/10.1086/301527)
- Hamuy, M., Phillips, M. M., Suntzeff, N. B., et al. 1996, *AJ*, 112, 2408, doi: [10.1086/118192](https://doi.org/10.1086/118192)
- Hamuy, M., Folatelli, G., Morrell, N. I., et al. 2006, *PASP*, 118, 2, doi: [10.1086/500228](https://doi.org/10.1086/500228)
- Hicken, M., Challis, P., Jha, S., et al. 2009, *ApJ*, 700, 331, doi: [10.1088/0004-637X/700/1/331](https://doi.org/10.1088/0004-637X/700/1/331)
- Hsiao, E. Y., Conley, A., Howell, D. A., et al. 2007, *ApJ*, 663, 1187, doi: [10.1086/518232](https://doi.org/10.1086/518232)
- Hsiao, E. Y., Phillips, M. M., Marion, G. H., et al. 2019, *PASP*, 131, 014002, doi: [10.1088/1538-3873/aae961](https://doi.org/10.1088/1538-3873/aae961)
- Joyce, A., Lombriser, L., & Schmidt, F. 2016, ArXiv e-prints. <https://arxiv.org/abs/1601.06133>
- Kelly, P. L., Filippenko, A. V., Burke, D. L., et al. 2015, *Science*, 347, 1459, doi: [10.1126/science.1261475](https://doi.org/10.1126/science.1261475)
- Kelly, P. L., Hicken, M., Burke, D. L., Mandel, K. S., & Kirshner, R. P. 2010, *ApJ*, 715, 743, doi: [10.1088/0004-637X/715/2/743](https://doi.org/10.1088/0004-637X/715/2/743)
- Krisciunas, K., Contreras, C., Burns, C. R., et al. 2017, *AJ*, 154, 211, doi: [10.3847/1538-3881/aa8df0](https://doi.org/10.3847/1538-3881/aa8df0)
- Lampeitl, H., Smith, M., Nichol, R. C., et al. 2010, *ApJ*, 722, 566, doi: [10.1088/0004-637X/722/1/566](https://doi.org/10.1088/0004-637X/722/1/566)
- Le Borgne, D., & Rocca-Volmerange, B. 2002, *A&A*, 386, 446, doi: [10.1051/0004-6361:20020259](https://doi.org/10.1051/0004-6361:20020259)
- Neill, J. D., Sullivan, M., Howell, D. A., et al. 2009, *ApJ*, 707, 1449, doi: [10.1088/0004-637X/707/2/1449](https://doi.org/10.1088/0004-637X/707/2/1449)
- Pan, Y.-C., Sullivan, M., Maguire, K., et al. 2014, *MNRAS*, 438, 1391, doi: [10.1093/mnras/stt2287](https://doi.org/10.1093/mnras/stt2287)
- Perlmutter, S., Gabi, S., Goldhaber, G., et al. 1997, *ApJ*, 483, 565
- Phillips, M. M. 1993, *ApJL*, 413, L105, doi: [10.1086/186970](https://doi.org/10.1086/186970)
- Phillips, M. M., Contreras, C., Hsiao, E. Y., et al. 2019, *PASP*, 131, 014001, doi: [10.1088/1538-3873/aae8bd](https://doi.org/10.1088/1538-3873/aae8bd)
- Pruzhinskaya, M., Novinskaya, A., Pauna, N., & Rosnet, P. 2020, arXiv e-prints, arXiv:2006.09433. <https://arxiv.org/abs/2006.09433>
- Rana, N. C., & Basu, S. 1992, *A&A*, 265, 499
- Riess, A. G., Filippenko, A. V., Challis, P., et al. 1998, *AJ*, 116, 1009, doi: [10.1086/300499](https://doi.org/10.1086/300499)
- Rigault, M., Copin, Y., Aldering, G., et al. 2013, *A&A*, 560, A66, doi: [10.1051/0004-6361/201322104](https://doi.org/10.1051/0004-6361/201322104)
- Roman, M., Hardin, D., Betoule, M., et al. 2018, *A&A*, 615, A68, doi: [10.1051/0004-6361/201731425](https://doi.org/10.1051/0004-6361/201731425)
- Schweizer, F., Burns, C. R., Madore, B. F., et al. 2008, *AJ*, 136, 1482, doi: [10.1088/0004-6256/136/4/1482](https://doi.org/10.1088/0004-6256/136/4/1482)
- Scolnic, D. M., Jones, D. O., Rest, A., et al. 2017, ArXiv e-prints. <https://arxiv.org/abs/1710.00845>
- Stritzinger, M. D., Phillips, M. M., Boldt, L. N., et al. 2011, *AJ*, 142, 156, doi: [10.1088/0004-6256/142/5/156](https://doi.org/10.1088/0004-6256/142/5/156)
- Sullivan, M., Conley, A., Howell, D. A., et al. 2010, *MNRAS*, 406, 782, doi: [10.1111/j.1365-2966.2010.16731.x](https://doi.org/10.1111/j.1365-2966.2010.16731.x)
- Tripp, R. 1998, *A&A*, 331, 815
- Uddin, S. A., Mould, J., Lidman, C., Ruhlmann-Kleider, V., & Hardin, D. 2017a, *PASA*, 34, e009, doi: [10.1017/pasa.2017.2](https://doi.org/10.1017/pasa.2017.2)
- Uddin, S. A., Mould, J., Lidman, C., Ruhlmann-Kleider, V., & Zhang, B. R. 2017b, *ApJ*, 848, 56, doi: [10.3847/1538-4357/aa8df7](https://doi.org/10.3847/1538-4357/aa8df7)
- Wang, L., Höflich, P., & Wheeler, J. C. 1997, *ApJL*, 483, L29, doi: [10.1086/310737](https://doi.org/10.1086/310737)
- Wiseman, P., Smith, M., Childress, M., et al. 2020, *MNRAS*, doi: [10.1093/mnras/staa1302](https://doi.org/10.1093/mnras/staa1302)